

Supporting Information

A set of highly sensitive sirtuin fluorescence probes for screening small-molecular SIRT defatty-acylase inhibitors

Yuya Nakajima, Mitsuyasu Kawaguchi*, Naoya Ieda and Hidehiko Nakagawa*

Graduate School of Pharmaceutical Sciences, Nagoya City University, 3-1 Tanabe-dori, Mizuho-ku, Nagoya, Aichi 467-8603, Japan

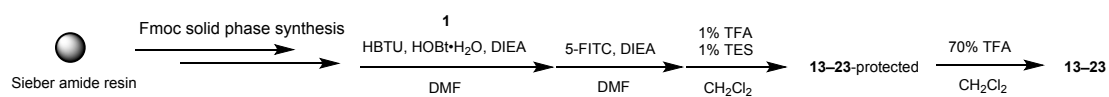
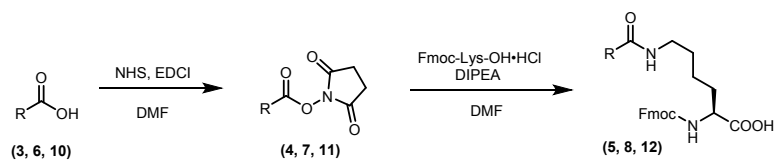
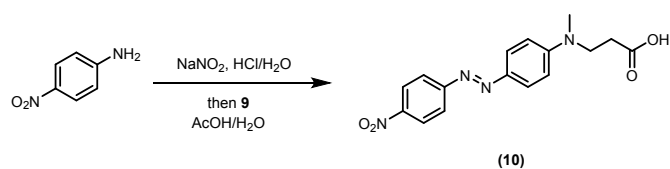
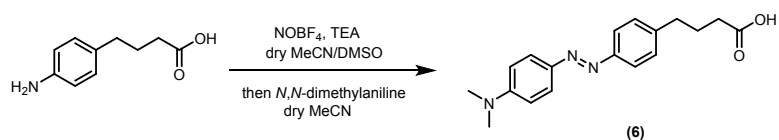
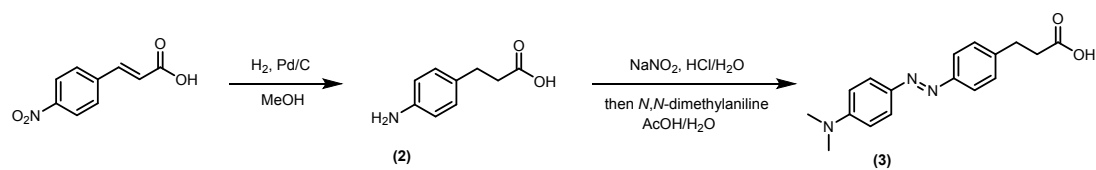
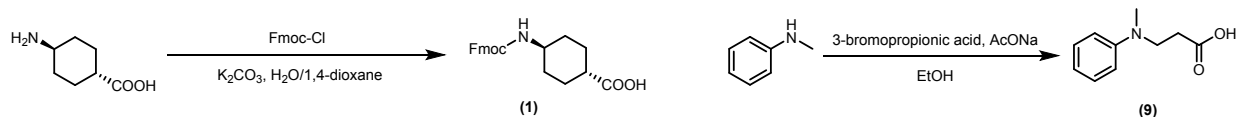
E-mail: mkawaguchi@phar.nagoya-cu.ac.jp, Tel: +81-52-836-3408 (M.K.)

E-mail: deco@phar.nagoya-cu.ac.jp, Tel: +81-52-836-3407 (H.N.)

Contents

Synthesis of quenchers with <i>L</i> -lysine (5 , 8 , 12), linker moiety (1) and SIRT probes (13–23) (Scheme S1).....	S3
Chemical structure of the one-step SIRT defatty-acylase probe SFP3 (Figure S1).....	S4
Enzymatic reaction of SFP3 and 13–23 with SIRT1–7 and effect of the SIRT inhibitor NAM (96-well microplate format) (Figure S2).....	S5
Michaelis-Menten plots for SFP3 and 13–23 with SIRT1 (Figure S3A)	S6
Michaelis-Menten plots for SFP3 and 13–23 with SIRT2 (Figure S3B)	S7
Michaelis-Menten plots for SFP3 and 13–23 with SIRT3 (Figure S3C)	S8
Docking models of Dabcyl-PH, Dabcyl-BH and Disperse Red with the SIRT2 catalytic site (Figure S4).....	S9
The interactions of the SIRT2 catalytic site with Dabcyl-PH. (Figure S5A).....	S10
The interactions of the SIRT2 catalytic site with Dabcyl-BH. (Figure S5B).....	S10
The interactions of the SIRT2 catalytic site with Disperse Red. (Figure S5C).....	S11
Chemical structures of peptide-based SIRT2 inhibitors, S2DMi-6 and S2DMi-9 and inhibition curve of S2DMi-9 toward SIRT6 obtained by using 23 (Figure S6).....	S12
Chemical structures of inhibitors A and B , and inhibition curves of A and B toward SIRT2 obtained by using the two-step defatty-acylase probe p53(My)-AMC (Figure S7).....	S13
Chemical structure of p53(My)-AMC and its detection mechanism of sirtuin activity (Figure S8).....	S13
Inhibitory activities of compound C toward defatty-acylase activity of SIRT1–3 and 6, and toward deacetylase activity of SIRT2 (Figure S9).....	S14
Inhibition curves of known small-molecular SIRT2 inhibitors toward SIRT2 using 18 (Figure S10).....	S14
k_{cat} values of enzymatic reactions of SIRT1–3 with SFP3 and 13–23 (Table S1A).....	S15
K_m values of enzymatic reactions of SIRT1–3 with SFP3 and 13–23 (Table S1B).....	S15
k_{cat}/K_m values of enzymatic reactions of SIRT1–3 with SFP3 and 13–23 (Table S1C).....	S16

General methods and materials.....	S16
Synthesis.....	S17
<i>In vitro</i> assay.....	S25
References for Supporting Information.....	S29



Scheme S1: Synthesis of quenchers with L-lysine (5, 8, 12), linker moiety (1) and SIRT probes (13–23).

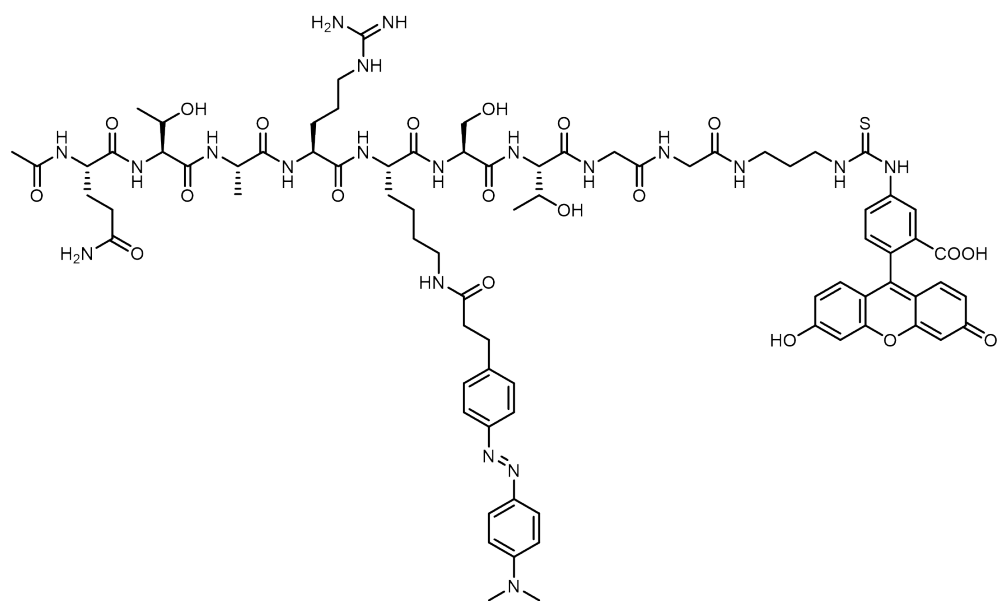


Figure S1: Chemical structure of the one-step SIRT defatty-acylase probe **SFP3^{S1}**.

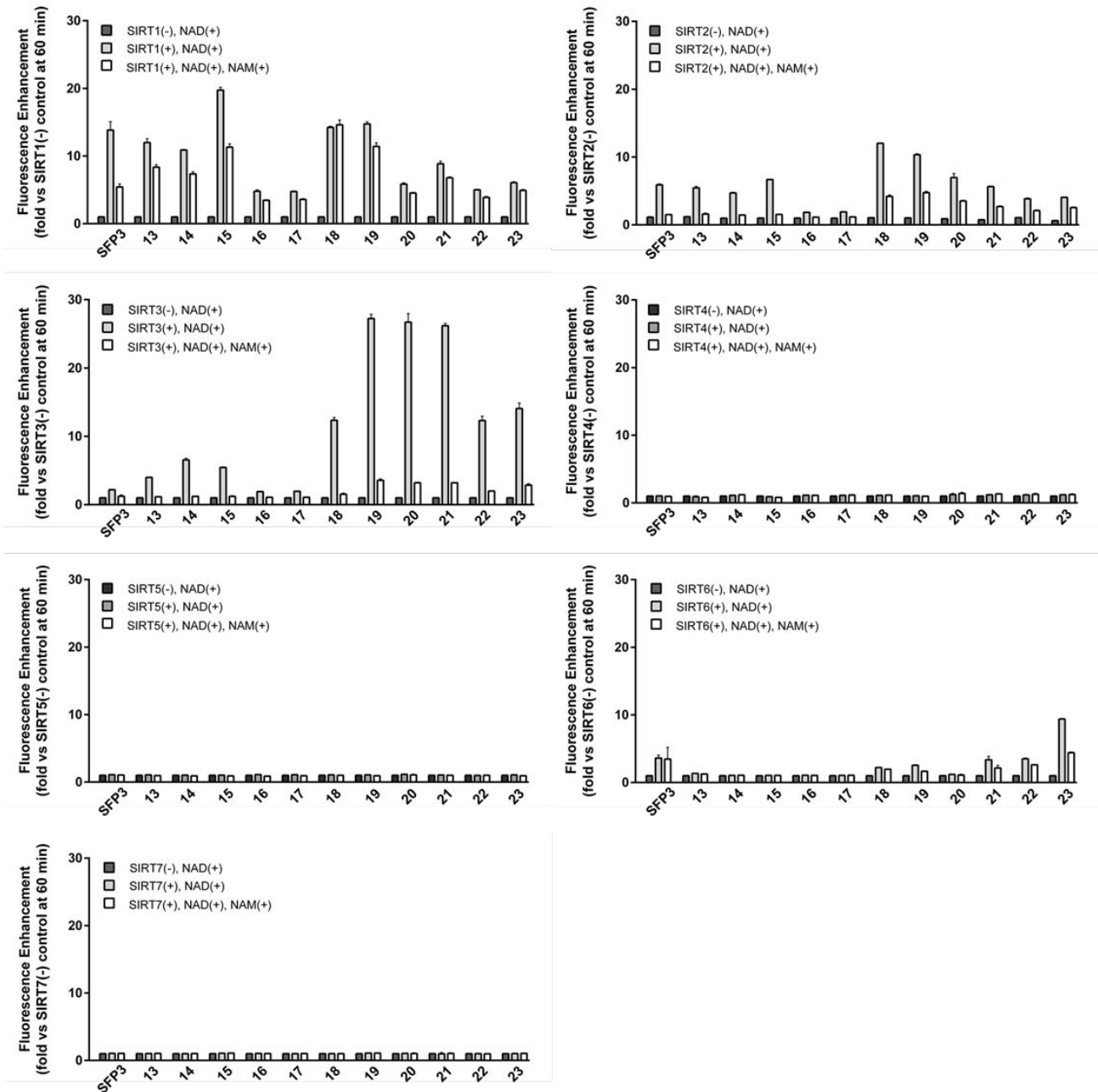


Figure S2: Enzymatic reaction of SFP3 and 13–23 with SIRT1–7 and effect of the SIRT inhibitor NAM (96-well microplate format).

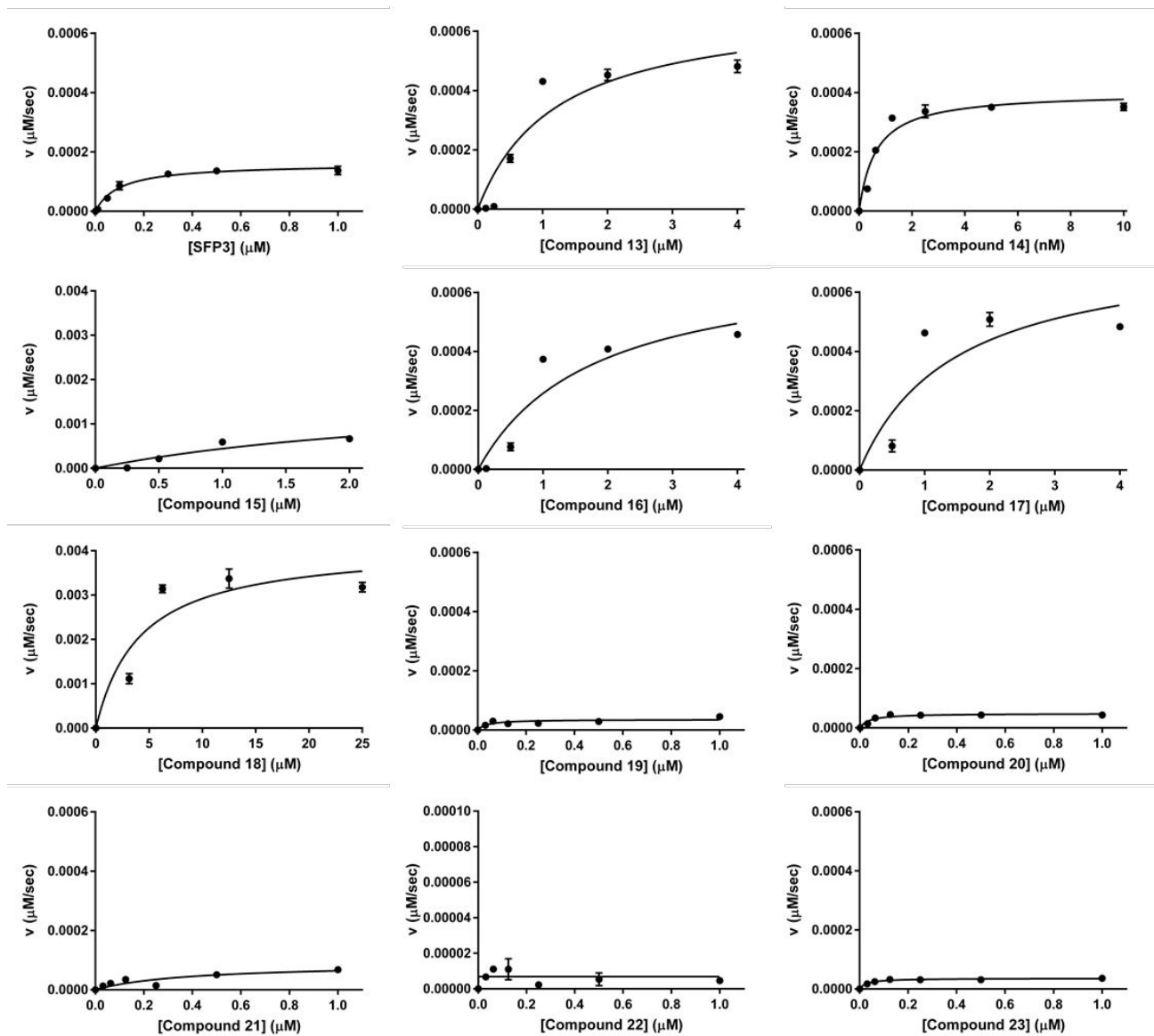


Figure S3A: Michaelis-Menten plots for SFP3 and 13–23 with SIRT1. Data for SFP3 were taken from (S1).

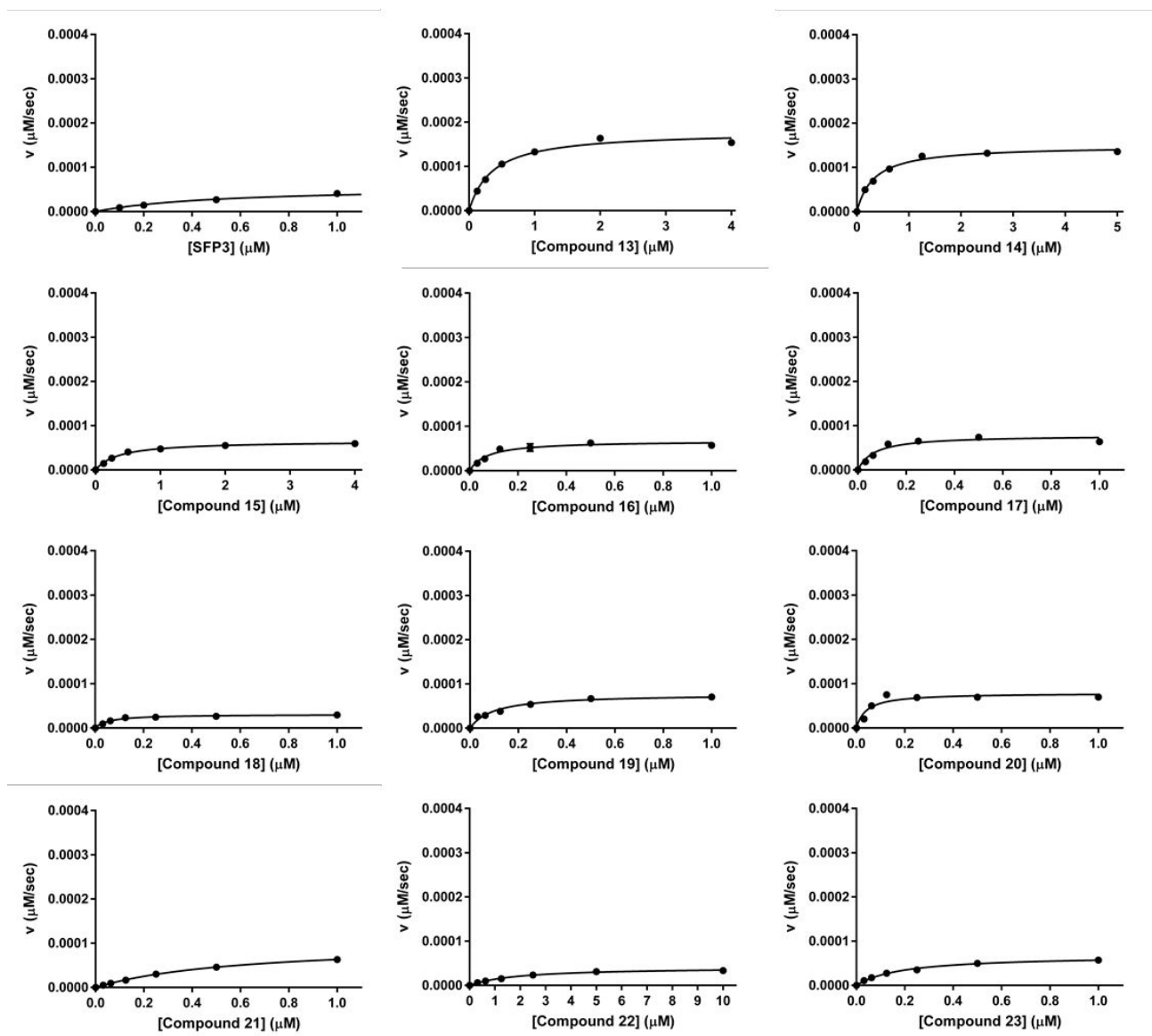


Figure S3B: Michaelis-Menten plots for **SFP3** and **13–23** with SIRT2. Data for **SFP3** were taken from (S1).

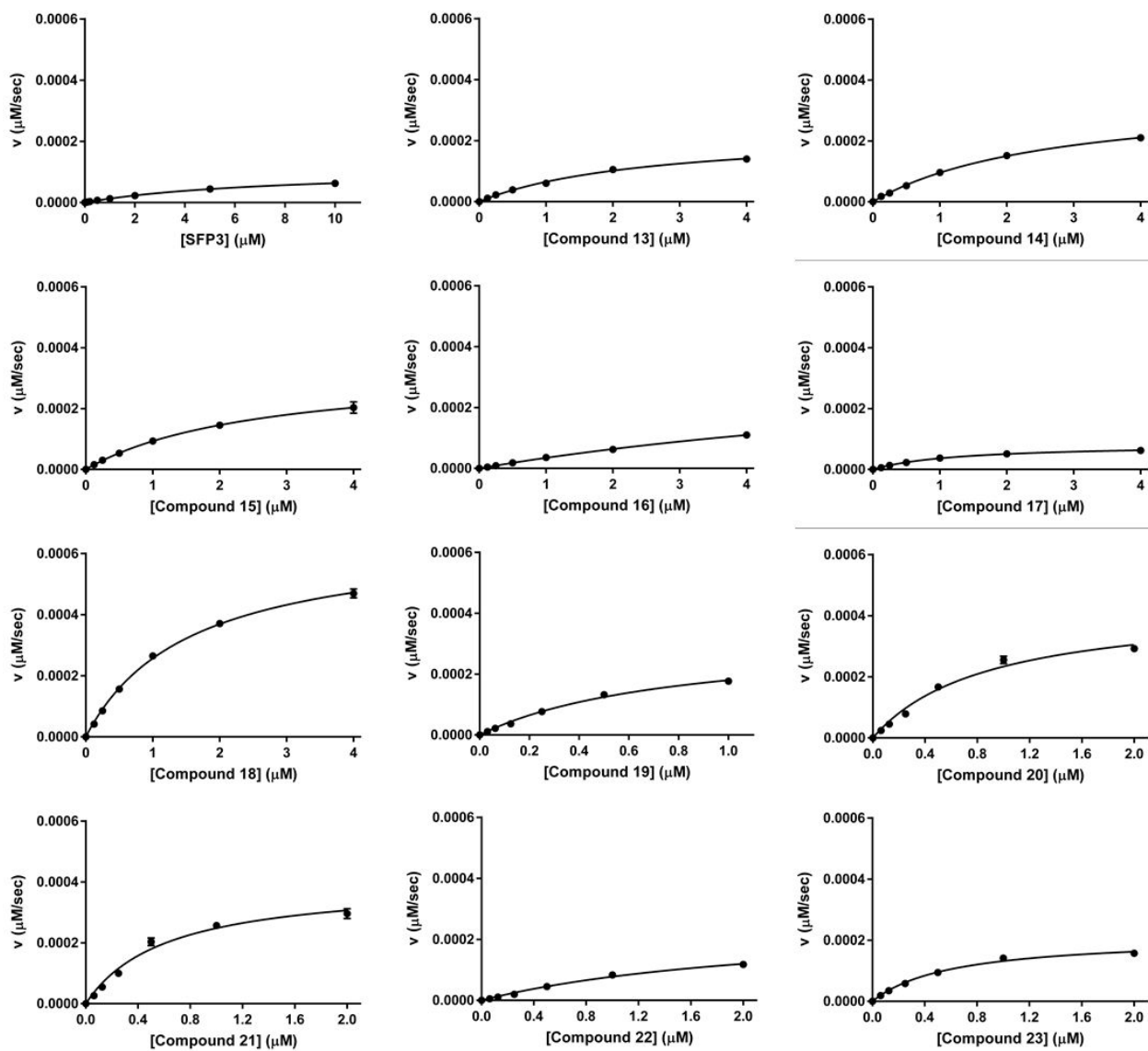
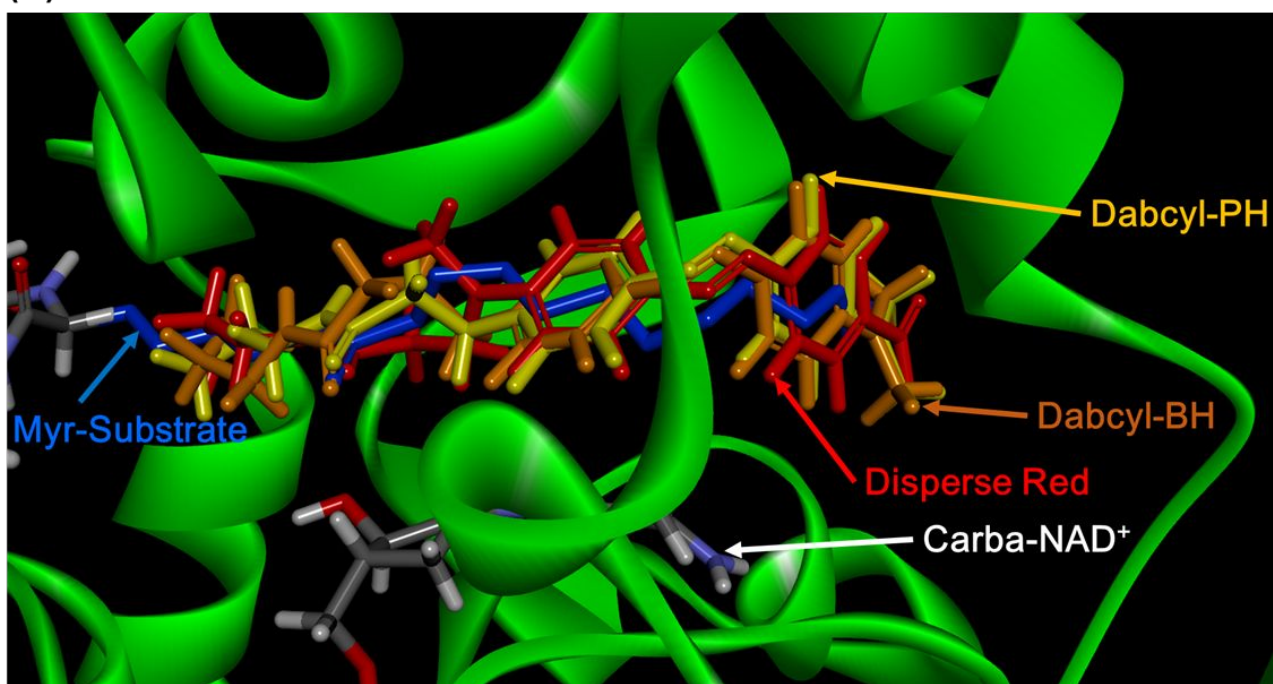


Figure S3C: Michaelis-Menten plots for SFP3 and 13–23 with SIRT3. Data for SFP3 were taken from (S1).

(A)



(B)

	CDOCKER interaction energy (kcal/mol)	CDOCKER energy (kcal/mol)
Dabcyl-PH	- 60.6158	- 54.4934
Dabcyl-BH	- 63.3286	- 57.0861
Disperse Red	- 63.8768	- 51.8617

Figure S4: (A) Docking models of Dabcyl-PH, Dabcyl-BH and Disperse Red with the SIRT2 catalytic site (PDB ID: 4X3P) using the CDOCKER algorithm in Discovery Studio Client v17.2.0.16349 (BIOVIA Inc.). (B) CDOCKER interaction energies (kcal/mol) and CDOCKER energies (kcal/mol) for the top ranked binding pose.

Dabcyl-PH

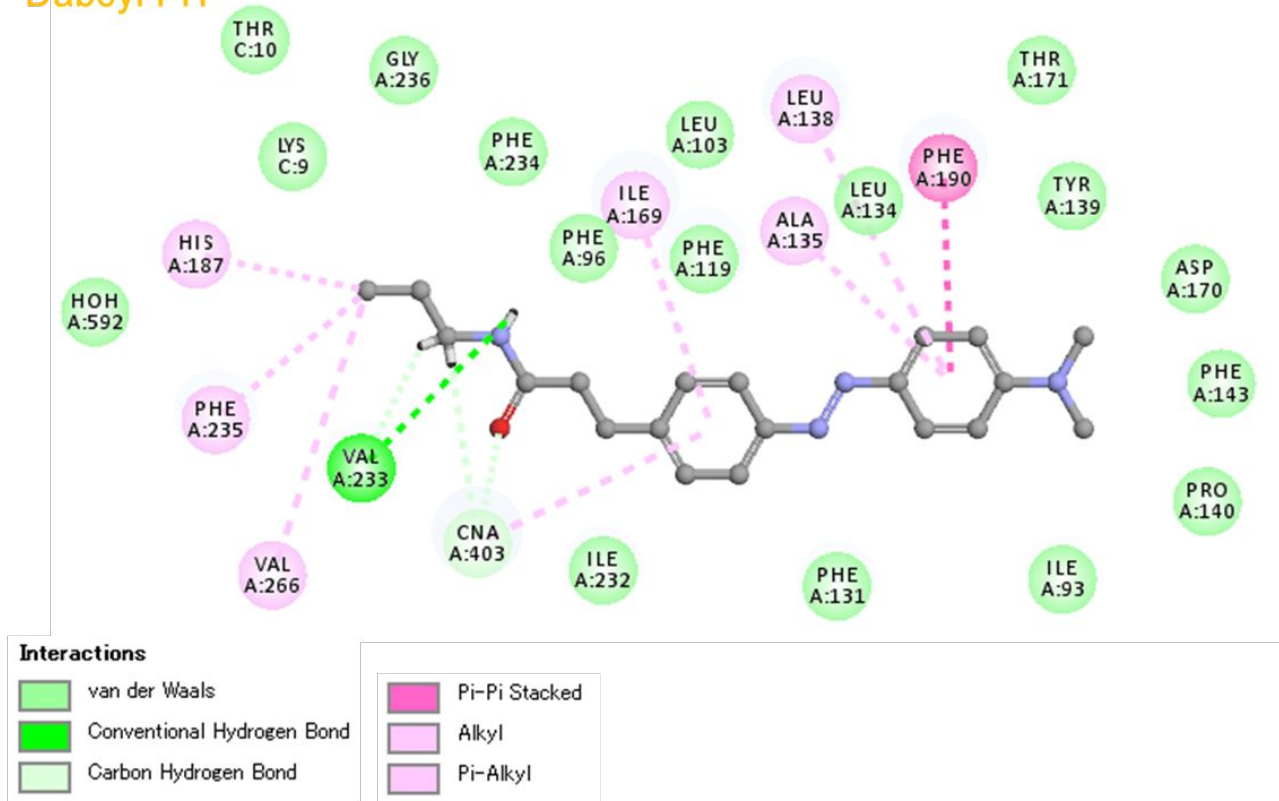


Figure S5A: The interactions of the SIRT2 catalytic site with Dabcyl-PH.

Dabcyl-BH

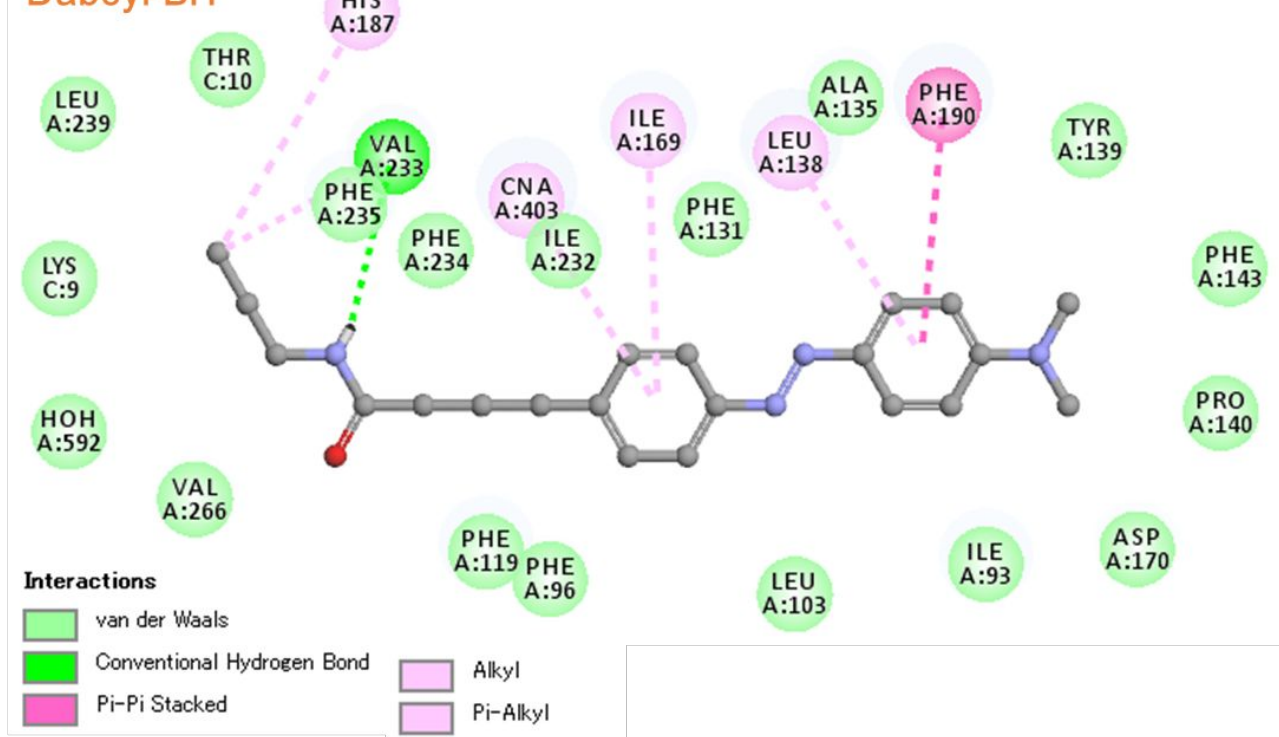


Figure S5B: The interactions of the SIRT2 catalytic site with Dabcyl-BH.

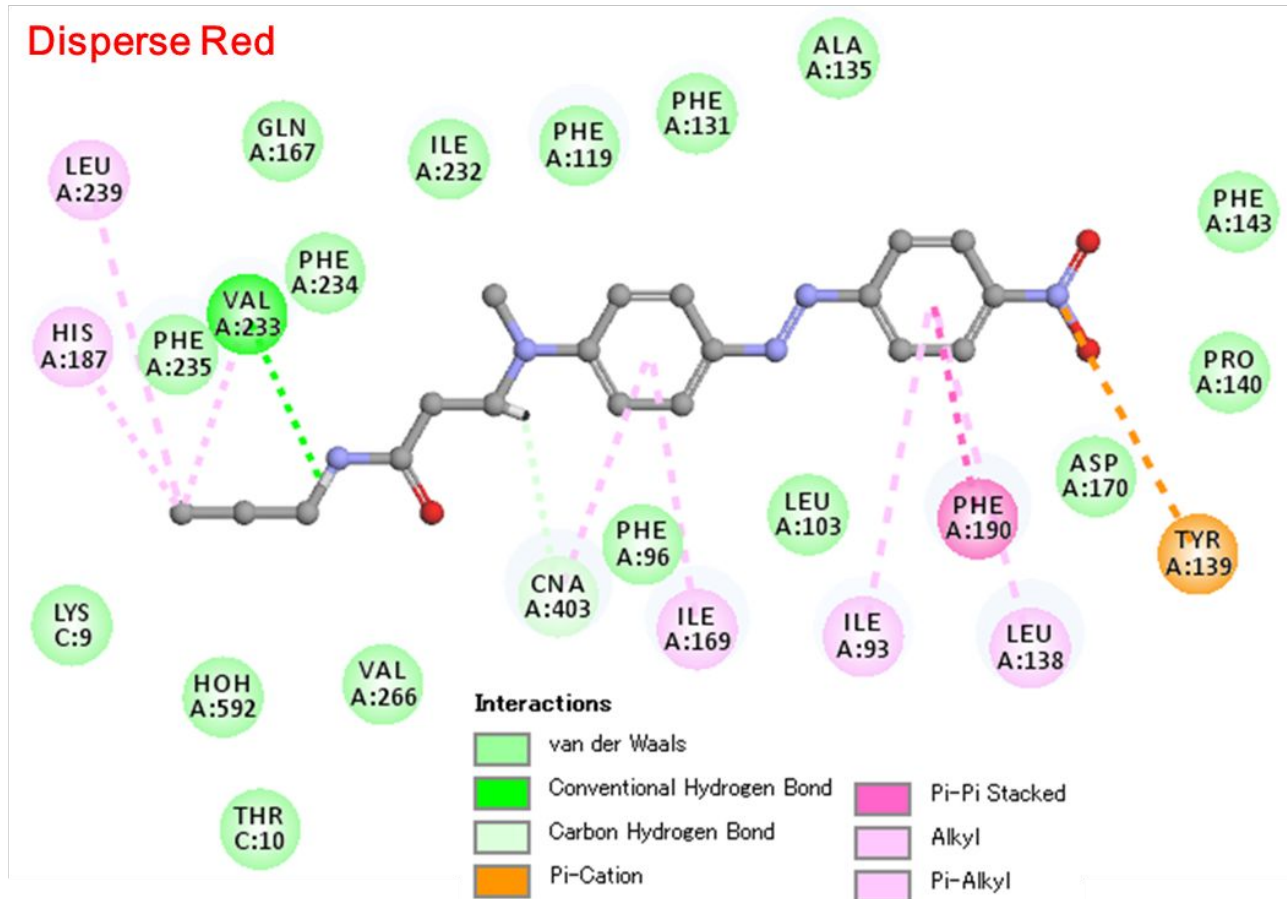


Figure S5C: The interactions of the SIRT2 catalytic site with Disperse Red.

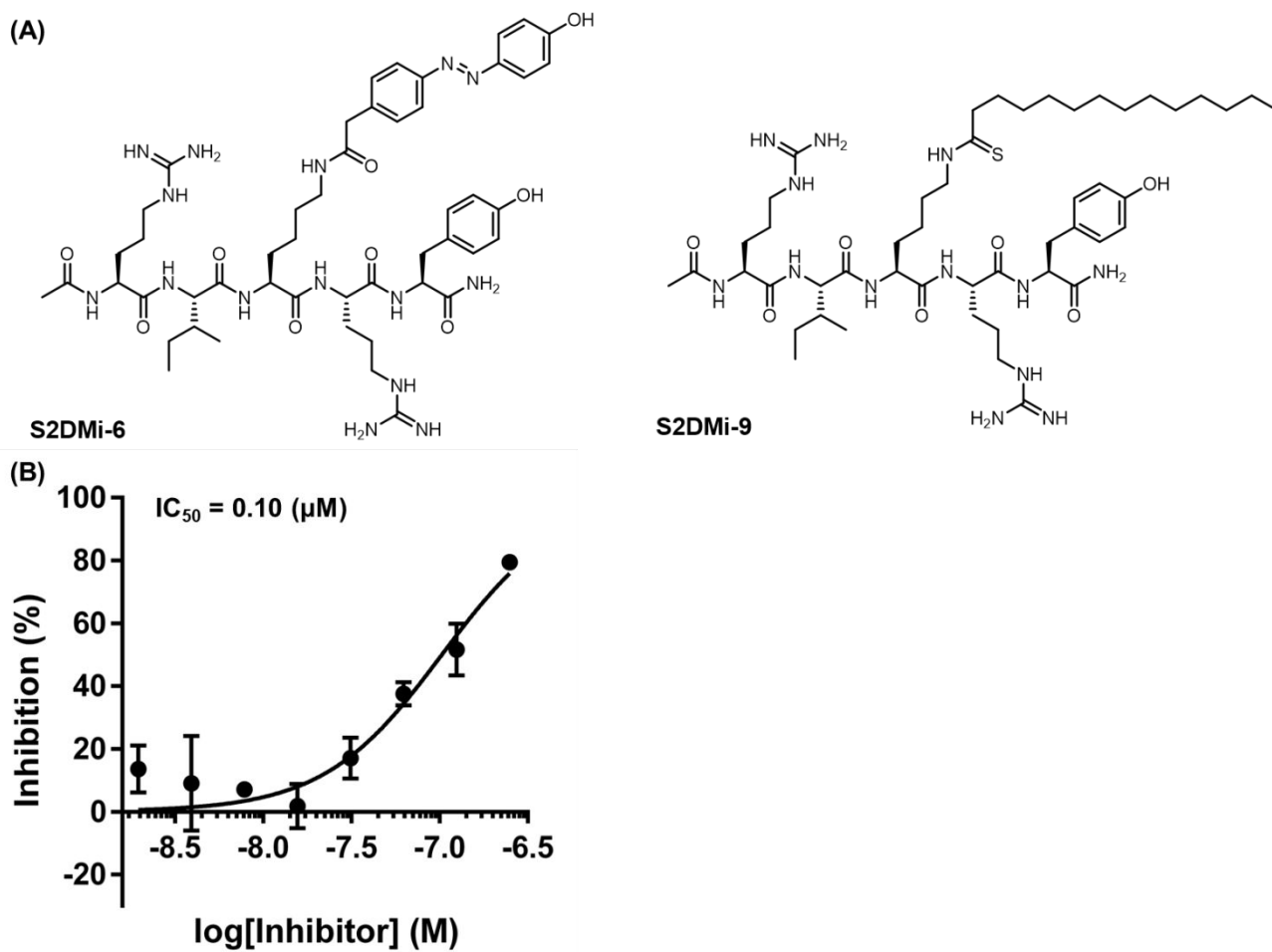


Figure S6: (A) Chemical structures of peptide-based SIRT2 inhibitors, **S2DMi-6** and **S2DMi-9**^{S6} (B) Inhibition curve of **S2DMi-9** toward SIRT6 obtained by using **23**. The results are mean \pm S.D. ($n = 3$).

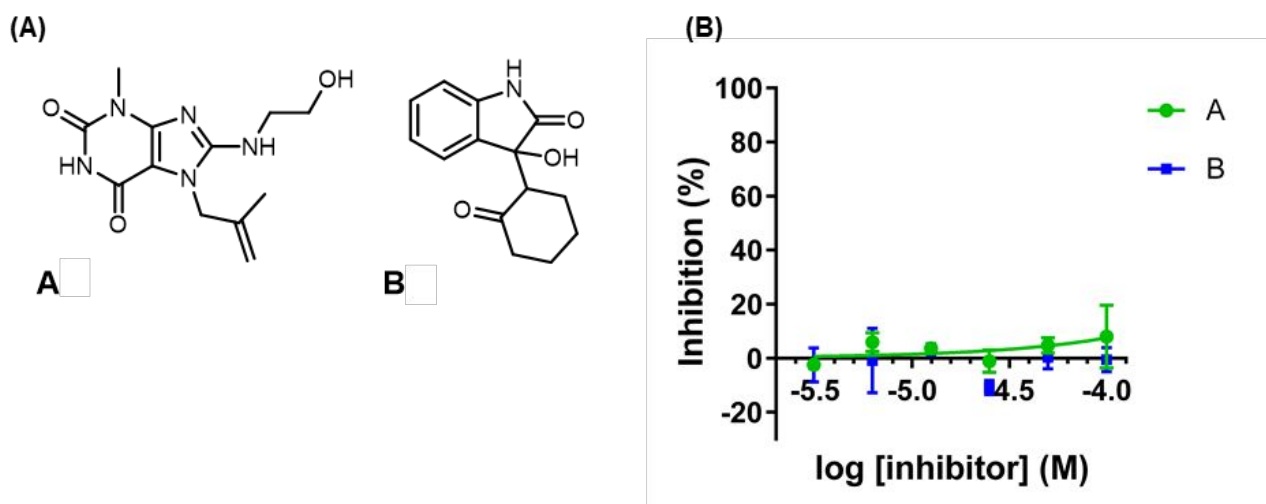


Figure S7: (A) Chemical structures of inhibitors A and B. (B) Inhibition curves of A and B toward SIRT2 obtained by using the two-step defatty-acylase probe **p53(Myristoyl)-AMC^{S6}**. The results are mean \pm S.D. ($n = 3$).

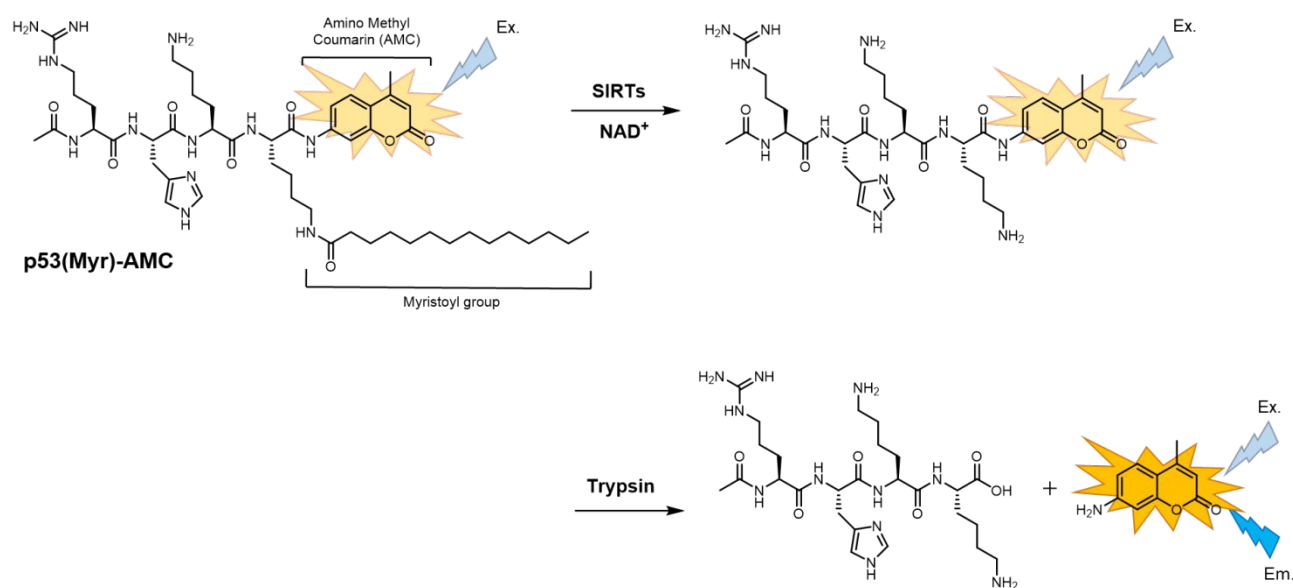


Figure S8: Chemical structure of **p53(Myristoyl)-AMC^{S6}** and its detection mechanism of sirtuin demyristoylase activity.

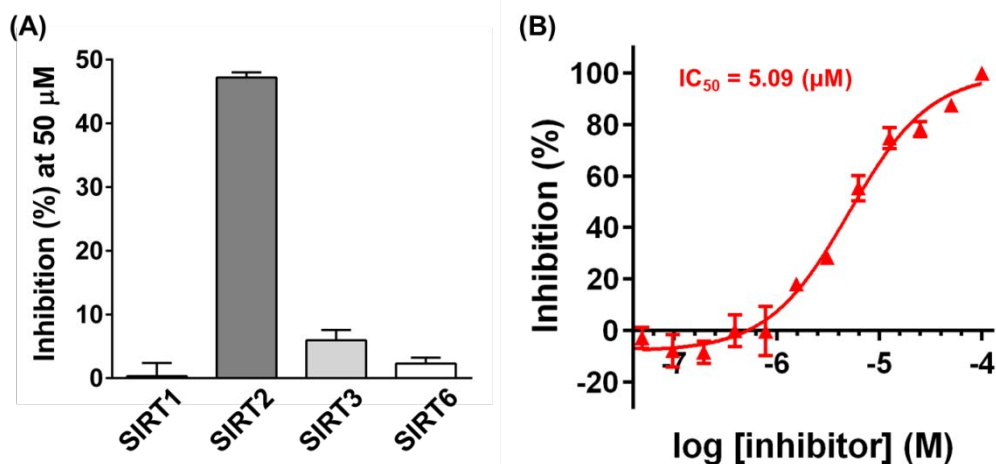
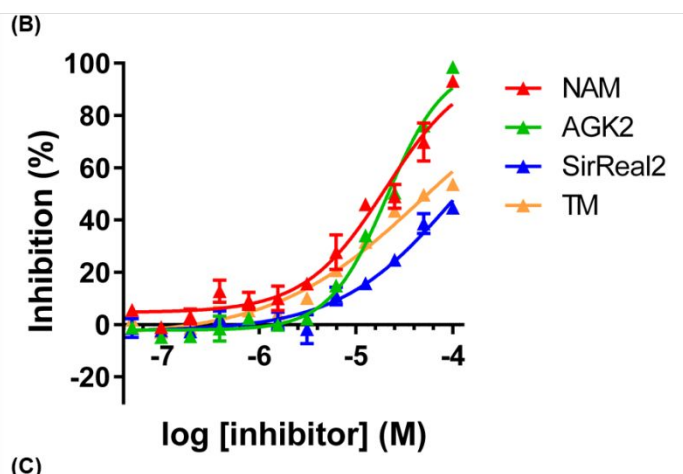
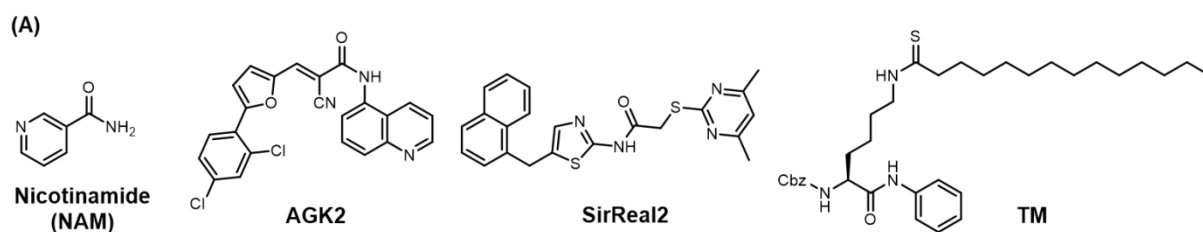


Figure S9: (A) Inhibitory activity (%) of compound **C** at the concentration of 50 μM toward SIRT1–3 obtained by using **18**, and toward SIRT6 obtained by using **23**. The results are mean \pm S.D. ($n = 3$). (B) Inhibition curve of compound **C** toward SIRT2 obtained with a **FLUOR DE LYS SIRT2 Kit**. The results are mean \pm S.D. ($n = 3$).



(C)

	SIRT2 (μM) 18	SIRT2 (μM) deAc
NAM	20 ± 1.2	$38 \pm 1.8^*$
AGK2	20 ± 1.0	$8.9 \pm 2.3^*$
SirReal2	>100	$0.70 \pm 0.061^*$
TM	47 ± 1.1	$0.14 \pm 0.014^*$
compound C	48 ± 1.3	5.1 ± 1.1

Figure S10: (A) Chemical structures of known small-molecular SIRT2 inhibitors, **nicotinamide**^{S2}, **AGK2**^{S3}, **SirReal2**^{S4}, and **TM**^{S5} (B) Inhibition curves of SIRT2 obtained by using **18**. The results are mean \pm S.D. ($n = 3$). (C)

IC₅₀ values for SIRT2 defatty-acylase activity (determined by using **18**) and for deacetylase activity. Asterisks indicate the IC₅₀ values were taken from (S6).

Table S1A: k_{cat} values of enzymatic reactions of SIRT1-3 with **SFP3** and **13–23**. Data for **SFP3** were taken from (S1).

	k_{cat} (s ⁻¹)		
	SIRT1	SIRT2	SIRT3
SFP3	0.023 ± 0.00085	0.0024 ± 0.000081	0.0019 ± 0.000027
13	0.039 ± 0.0052	0.010 ± 0.00024	0.013 ± 0.00059
14	0.023 ± 0.0010	0.0085 ± 0.00013	0.020 ± 0.00065
15	0.11 ± 0.043	0.0037 ± 0.000072	0.019 ± 0.00097
16	0.041 ± 0.0071	0.0038 ± 0.00017	0.023 ± 0.0026
17	0.043 ± 0.0084	0.0045 ± 0.00021	0.0048 ± 0.00016
18	0.24 ± 0.027	0.0018 ± 0.000037	0.037 ± 0.00072
19	0.0020 ± 0.00020	0.0044 ± 0.00015	0.018 ± 0.0010
20	0.0028 ± 0.00013	0.0045 ± 0.00023	0.025 ± 0.0014
21	0.0051 ± 0.00095	0.0058 ± 0.00012	0.023 ± 0.0011
22	N.D.	0.0024 ± 0.000067	0.015 ± 0.0012
23	0.0021 ± 0.000051	0.0039 ± 0.000079	0.012 ± 0.00043

Table S1B: K_m values of enzymatic reactions of SIRT1-3 with **SFP3** and **13–23**. Data for **SFP3** were taken from (S1).

	K_m (μM)		
	SIRT1	SIRT2	SIRT3
SFP3	0.10 ± 0.014	0.52 ± 0.058	7.7 ± 0.21
13	1.2 ± 0.39	0.36 ± 0.030	2.6 ± 0.22
14	0.63 ± 0.11	0.33 ± 0.020	2.7 ± 0.16
15	3.2 ± 1.9	0.36 ± 0.025	2.6 ± 0.25
16	1.8 ± 0.67	0.073 ± 0.012	11 ± 1.6
17	1.5 ± 0.66	0.068 ± 0.012	1.3 ± 0.10
18	4.1 ± 1.6	0.057 ± 0.0049	1.6 ± 0.067
19	0.038 ± 0.018	0.099 ± 0.011	0.80 ± 0.080
20	0.037 ± 0.0082	0.041 ± 0.0098	0.88 ± 0.11
21	0.39 ± 0.16	0.61 ± 0.024	0.62 ± 0.075
22	N.D.	1.9 ± 0.15	2.4 ± 0.30
23	0.029 ± 0.0038	0.19 ± 0.011	0.61 ± 0.053

Table S1C: k_{cat}/K_m values of enzymatic reactions of SIRT1-3 with SFP3 and 13–23. Data for SFP3 were taken from (S1).

	k_{cat}/K_m ($\text{M}^{-1}\text{s}^{-1}$)		
	SIRT1	SIRT2	SIRT3
SFP3	2.3×10^5	4.5×10^3	2.4×10^2
13	3.3×10^4	2.8×10^4	5.2×10^3
14	3.7×10^4	2.6×10^4	7.5×10^3
15	3.3×10^4	1.0×10^4	7.3×10^3
16	2.3×10^4	5.2×10^4	2.2×10^3
17	3.0×10^4	6.6×10^4	3.7×10^3
18	5.7×10^4	3.1×10^4	2.4×10^4
19	5.3×10^4	4.5×10^4	2.3×10^4
20	7.4×10^4	1.1×10^5	2.9×10^4
21	1.3×10^4	9.6×10^3	3.7×10^4
22	N.D.	1.2×10^3	6.3×10^3
23	7.1×10^4	2.0×10^4	2.0×10^4

[Experimental Section]

General methods and materials

Proton nuclear magnetic resonance spectra (^1H NMR) were recorded on a JEOL JNM-ECZ500 in the indicated solvent. Chemical shifts (δ) are reported in parts per million relative to internal standard tetramethylsilane (TMS). High-resolution mass spectra (HR-MS) were recorded on a JEOL JMS-SX102A. Purity was evaluated by analytical HPLC on a Shimadzu instrument equipped with a reversed-ODS column (Inertsil ODS-3 4.6×150 mm, GL Science, Tokyo, Japan) at flow rate of 1.0 mL min^{-1} . Semipreparative HPLC purification was performed with a JASCO PU-2086 pump system equipped with reverse-phase ODS column (Inertsil ODS-3 20×250 mm, GL Science) at flow rate of 10 mL min^{-1} . Ultraviolet-visible-light absorption spectra and fluorescence spectra were recorded on a UV-1800 (Shimadzu, Kyoto, Japan) and an RF5300-PC (Shimadzu), respectively. The fluorometer slit width was 5.0 nm for both excitation and emission, and the sensitivity was set to low. Microplate fluorescence assay were performed with an ARVO-X5 plate reader (PerkinElmer). Recombinant human sirtuins were purchased from the following companies: SIRT1 and 2 (R&D Systems), SIRT3 (ATGen), SIRT4, 5, 6 and 7 (BioVision). All other reagents and solvents were purchased from Sigma Aldrich (St. Louis, USA), Tokyo Chemical Industry Co., Ltd. (Tokyo, Japan), FUJIFILM Wako Pure Chemical Corporation (Osaka, Japan), Nacalai Tesque, Inc. (Kyoto, Japan), Kanto Chemical Co., Inc. (Tokyo, Japan), Kishida Chemical Co., Ltd. (Osaka, Japan) and Watanabe Chemical Industries, Ltd. (Hiroshima, Japan), and used without purification. Flash column chromatography was performed using Silica Gel 60 (particle size $0.046\text{--}0.063 \text{ mm}$) supplied by Taikoh-Shoji (Aichi, Japan).

Synthesis

Synthesis of 1

To a solution of *trans*-4-aminocyclohexanecarboxylic acid (0.10 g, 0.71 mmol, 1.0 eq.) in H₂O (2.6 mL) and 1,4-dioxane (1.0 mL) were added K₂CO₃ (0.36 g, 2.6 mmol, 3.8 eq.) and 9-fluorenylmethyl chloroformate (0.18 g, 0.68 mmol, 1.0 eq.) on ice. The mixture was stirred on ice for 5 hr, and at room temperature for 16 hr, and then H₂O (0.20 L) was added. The aqueous solution was extracted with diethyl ether three times. The aqueous layer was separated and acidified to pH 2 with 2 N HCl (4.0 mL), then cooled on ice. The precipitate was collected by filtration, washed with cold H₂O, and dried *in vacuo* to afford **1** (0.15 g, 0.42 mmol) as a white solid in 59% yield. ¹H-NMR (500 MHz, DMSO-*d*₆): δ 7.89 (d, 2H, *J* = 7.6 Hz), 7.69 (d, 2H, *J* = 7.5 Hz), 7.42 (t, 2H, *J* = 7.6 Hz), 7.33 (t, 2H, *J* = 7.5 Hz), 7.23 (d, 1H, *J* = 7.7 Hz), 4.27 (d, 2H, *J* = 6.9 Hz), 4.20 (t, 1H, *J* = 6.6 Hz), 3.21 (m, 1H), 2.08 (m, 1H), 1.88 (d, 2H, *J* = 14 Hz), 1.80 (d, 2H, *J* = 10 Hz), 1.32 (q, 2H, *J* = 13 Hz), 1.18 (q, 2H, *J* = 12 Hz); MS (ESI⁺): calcd for C₂₂H₂₃NO₄Na: m/z 388.2; found: m/z = 388.2 ([M+Na]⁺).

Synthesis of 2

To a solution of (*E*)-3-(4-nitrophenyl)acrylic acid (**1**) (3.1 g, 16 mmol, 1.0 eq.) in MeOH (20 mL) was added Pd/C (0.17 g, 0.16 mmol, 0.010 eq.). The reaction mixture was stirred under a H₂ balloon at room temperature for 4 hr, and then filtered through Celite. The filtrate was evaporated *in vacuo* to afford **2** (2.5 g, 15 mmol) as a reddish brown solid in 94% yield. ¹H-NMR (500 MHz, DMSO-*d*₆): δ 6.85 (d, 2H, *J* = 8.6 Hz), 6.47 (d, 2H, *J* = 8.5 Hz), 2.63 (t, 2H, *J* = 7.9 Hz), 2.41 (t, 2H, *J* = 7.9 Hz); MS (ESI⁺): calcd for C₉H₁₂NO₂: m/z 166.1; found: 166.1 ([M+H]⁺).

Synthesis of 3

To a solution of **2** (2.5 g, 15 mmol, 1.0 eq.) in 1 N HCl (50 mL) was added NaNO₂ (1.0 g, 15 mmol, 1.0 eq.). The reaction mixture was stirred on ice for 1.5 hr, then a solution of *N,N*-dimethylaniline (2.3 mL, 18 mmol, 1.2 eq.) in AcOH (6.0 mL) and H₂O (3.0 mL) was added on ice. The reaction mixture was stirred on ice for 1 hr, then basified to pH = 4 with 2 N NaOH and sodium phosphate buffer. The resulting precipitate was collected by filtration and dried *in vacuo* to afford **3** (3.0 g, 11 mmol) as a reddish brown solid in 74% yield. ¹H-NMR (500 MHz, CDCl₃): δ 7.87 (d, 2H, *J* = 9.1 Hz), 7.78 (d, 2H, *J* = 8.5 Hz), 7.32 (d, 2H, *J* = 8.3 Hz), 6.76 (d, 2H, *J* = 9.2 Hz), 3.09 (s, 6H), 3.03 (t, 2H, *J* = 7.8 Hz), 2.73 (t, 2H, *J* = 8.0 Hz).

Synthesis of 4

To a solution of **3** (3.0 g, 11 mmol, 1.0 eq.) and EDCI (0.43 g, 22 mmol, 2.0 eq.) in dry DMF (50 mL) was added *N*-hydroxysuccinimide (0.26 g, 22 mmol, 2.0 eq.). The reaction mixture was stirred at room temperature for 16 hr, and then AcOEt was added. The organic layer was washed three times with sodium phosphate buffer (pH ~ 4) and once with brine, dried over Na₂SO₄, and evaporated *in vacuo*. The residue was purified by column chromatography on silica gel (eluent: *n*-hexane/AcOEt = 2/1 → 1/1 → 1/2 → 1/4 → 1/8 → AcOEt only) to afford **4** (0.17 g, 4.3 mmol) as an orange solid in 38% yield. ¹H-NMR (500 MHz, CDCl₃): δ 7.87 (d, 2H, *J* = 9.1 Hz), 7.80 (d, 2H, *J* = 8.5 Hz), 7.33 (d, 2H, *J* = 8.4 Hz), 6.76 (d, 2H, *J* = 9.1 Hz), 3.12 (t, 2H, *J* = 8.5 Hz), 3.09 (s, 6H), 2.96 (t, 2H, *J* = 8.5 Hz), 2.85 (s, 4H).

Synthesis of 5

To a solution of Fmoc-Lys-OH·HCl (1.9 g, 4.7 mmol, 1.1 eq.) and DIEA (4.5 mL, 26 mmol, 6.0 eq.) in DMF (6.0 mL) was added **4** (1.7 g, 4.3 mmol, 1.0 eq.) in DMF (30 mL). The reaction mixture was stirred at room temperature for 2 hr, and then AcOEt was added. The organic layer was washed three times with sodium phosphate buffer (pH ~ 4) and once with brine, dried over Na₂SO₄, and evaporated *in vacuo*. The residue was purified by column chromatography on silica gel (eluent: CH₂Cl₂/MeOH = 97/3→95/5→92/8→9/1→7/3→MeOH only) to afford **5** (21 g, 3.2 mmol) as a red solid in 76% yield. ¹H-NMR (500 MHz, CDCl₃): δ 7.86 (d, 2H, *J* = 8.7 Hz), 7.75 (d, 2H, *J* = 7.5 Hz), 7.69 (d, 2H, *J* = 8.0 Hz), 7.60 (d, 2H, *J* = 7.3 Hz), 7.39 (t, 2H, *J* = 7.4 Hz), 7.29 (m, 4H), 6.73 (d, 2H, *J* = 9.1 Hz), 4.38 (m, 2H), 4.21 (t, 1H, *J* = 7.3 Hz), 3.30 (m, 1H), 3.19–2.97 (m, 10H), 2.48 (m, 2H), 1.90–1.68 (m, 2H), 1.45–1.36 (m, 2H), 1.28–1.08 (m, 2H).

Synthesis of 6

To a solution of 4-(4-aminophenyl)butanoic acid (0.30 g, 1.7 mmol, 1.0 eq.) in dry MeCN/DMSO (4.0/1.0 mL) on ice were added TEA (0.25 mL, 1.8 mmol, 1.1 eq.) and NOBF₄ (0.44 g, 3.7 mmol, 2.3 eq.). The reaction mixture was stirred on ice for 15 min, then *N,N*-dimethylaniline (0.50 mL, 4.0 mmol, 2.4 eq.) in dry MeCN (20 mL) was added. The reaction mixture was further stirred on ice for 15 min, and at room temperature for 30 min, then evaporated *in vacuo*. The residue was purified by column chromatography on silica gel (eluent: *n*-hexane/AcOEt = 1/2) twice to afford **6** (0.41 g, 1.3 mmol) as a reddish brown solid in 79% yield. ¹H-NMR (500 MHz, CDCl₃): δ 7.87 (d, 2H, *J* = 9.2 Hz), 7.77 (d, 2H, *J* = 8.5 Hz), 7.29 (d, 2H, *J* = 8.2 Hz), 6.76 (d, 2H, *J* = 9.2 Hz), 3.09 (s, 6H), 2.75 (t, 2H, *J* = 7.6 Hz), 2.40 (t, 2H, *J* = 7.4 Hz), 2.01 (t, 2H, *J* = 7.6 Hz); MS (ESI⁺): calcd for C₁₈H₂₂N₃O₂: *m/z* 312.2; found: 312.2 ([M+H]⁺).

Synthesis of 8

To a solution of **6** (0.41 g, 1.3 mmol, 1.0 eq.) and EDCI·HCl (1.3 g, 6.5 mmol, 5.0 eq.) in dry DMF (12 mL) was added *N*-hydroxysuccinimide (0.75 g, 6.5 mmol, 5.0 eq.). The reaction mixture was stirred at room temperature for 5 hr, and then AcOEt was added. The organic layer was washed three times with sodium phosphate buffer (pH ~ 4) and once with brine, dried over Na₂SO₄, and evaporated *in vacuo*. The residue was purified by column chromatography on silica gel (eluent: *n*-hexane/AcOEt = 1/1) to afford crude **7** (0.36 g) as an orange solid. ¹H-NMR (500 MHz, CDCl₃): δ 7.87 (d, 2H, *J* = 9.1 Hz), 7.78 (d, 2H, *J* = 8.5 Hz), 7.29 (d, 2H, *J* = 8.4 Hz), 6.76 (d, 2H, *J* = 9.2 Hz), 3.09 (s, 6H), 2.85 (s, 4H), 2.80 (t, 2H, *J* = 7.7 Hz), 2.64 (t, 2H, *J* = 7.2 Hz), 2.11 (m, 2H); MS (ESI⁺): calcd for C₂₂H₂₅N₄O₄: *m/z* 409.2; found: 409.2 ([M+H]⁺).

To a solution of crude **7** (0.36 g, 0.89 mmol, 1.0 eq.) and DIEA (0.46 mL, 2.7 mmol, 3.0 eq.) in DMF (8.0 mL) was added Fmoc-Lys-OH·HCl (0.43 g, 1.1 mmol, 1.2 eq.). The reaction mixture was stirred at room temperature for 2.5 hr, and then AcOEt was added. The organic layer was washed three times with sodium phosphate buffer (pH ~ 4) and once with brine, dried over Na₂SO₄, and evaporated *in vacuo*. The residue was purified by column chromatography on silica gel (eluent: CH₂Cl₂/MeOH = 99/1→97/3→92/8→9/1) to afford **8** (0.52 g, 0.79 mmol) as a red solid in 61% yield. ¹H-NMR (500 MHz, CDCl₃): δ 7.85 (d, 2H, *J* = 9.1 Hz), 7.74 (m, 4H), 7.59 (t, 2H, *J* = 7.2

Hz), 7.38 (t, 2H, $J = 7.5$ Hz), 7.29 (m, 2H), 7.25 (m, 2H), 6.75 (d, 2H, $J = 9.1$ Hz), 4.38 (m, 3H), 4.21 (m, 1H), 3.40–3.15 (m, 2H), 3.07 (s, 6H), 2.64 (m, 2H), 2.17 (m, 2H), 2.00–1.75 (m, 2H), 1.70–1.45 (m, 6H), 1.45–1.30 (m, 2H); MS (ESI⁺): calcd for C₃₉H₄₄N₅O₅: m/z 662.3; found: 662.4 ([M+H]⁺).

Synthesis of 9

To a solution of *N*-methylaniline (2.2 mL, 20 mmol, 2.0 eq.) in EtOH (30 mL) were added 3-bromopropionic acid (1.5 g, 10 mmol, 1.0 eq.) and AcONa (1.6 g, 20 mmol, 2.0 eq.). The reaction mixture was stirred at reflux temperature for 5 hr, and at room temperature overnight. The mixture was diluted with H₂O, then NaOH aq. was added, and the whole was washed five times with Et₂O (30 mL). The aqueous layer was acidified with HCl aq. (pH ~ 5) and extracted with Et₂O. The organic layer was evaporated *in vacuo*. The residue was purified by column chromatography on silica gel (eluent: CH₂Cl₂/MeOH = 98/2 → 97/3) to afford **9** (0.93 g, 5.2 mmol) as a white solid in 52% yield. ¹H-NMR (500 MHz, CD₃OD): δ 7.27–7.24 (m, 2H), 6.80–6.77 (m, 3H), 3.65 (t, 2H, $J = 7.0$ Hz), 2.94 (s, 3H), 2.62 (t, 2H, $J = 7.1$ Hz).

Synthesis of 10

To a solution of 4-nitroaniline (0.65 g, 4.7 mmol, 1.0 eq.) in 1 N HCl (30 mL) was added NaNO₂ (0.39 g, 5.6 mmol, 1.2 eq.). The reaction mixture was stirred on ice for 30 min, and then a solution of compound **9** (0.93 mg, 5.2 mmol, 1.1 eq.) in AcOH (20 mL) and H₂O (10 mL) was added. The reaction mixture was stirred on ice for 5 min, and at room temperature for 2 hr, then 2 N NaOH aq. (15 mL) was added to adjust the pH to ~ 4. The formed precipitate was collected by filtration, washed with H₂O, and dried *in vacuo* to afford **10** (1.2 g, 3.5 mmol) as a red solid in 75% yield. ¹H-NMR (500 MHz, CD₃OD): δ 8.36 (d, 2H, $J = 8.8$ Hz), 7.94 (d, 2H, $J = 9.1$ Hz), 7.86 (t, 2H, $J = 9.2$ Hz), 6.90 (t, 2H, $J = 9.3$ Hz), 3.75 (d, 2H, $J = 7.1$ Hz), 3.08 (s, 3H), 2.56 (t, 2H, $J = 7.2$ Hz).

Synthesis of 11

To a solution of **10** (0.66 g, 2.0 mmol, 1.0 eq.) and EDCI (0.76 g, 4.0 mmol, 2.0 eq.) in dry DMF (6.0 mL) was added *N*-hydroxysuccinimide (0.46 g, 4.0 mmol, 2.0 eq.). The reaction mixture was stirred at room temperature for 1 hr, and then AcOEt was added. The organic layer was washed three times with sodium phosphate buffer (pH ~ 4) and once with brine, dried over Na₂SO₄, and evaporated *in vacuo*. The residue was purified by column chromatography on silica gel (eluent: *n*-hexane/AcOEt = 1/1 → 1/2 → 1/3) to afford **11** (0.22 g, 0.51 mmol) as a red solid in 26% yield. ¹H-NMR (500 MHz, CD₃OD): δ 8.37 (d, 2H, $J = 9.2$ Hz), 7.96 (d, 2H, $J = 9.1$ Hz), 7.88 (t, 2H, $J = 9.3$ Hz), 6.95 (t, 2H, $J = 9.3$ Hz), 3.90 (t, 2H, $J = 6.8$ Hz), 3.11 (s, 3H), 3.03 (t, 2H, $J = 6.7$ Hz), 2.82 (m, 4H).

Synthesis of 12

To a solution of Fmoc-Lys-OH·HCl (0.22 g, 0.54 mmol, 1.1 eq.) and DIEA (0.27 mL, 1.5 mmol, 3.0 eq.) in DMF (5.0 mL) was added **11** (0.22 g, 0.51 mmol, 1.0 eq.). The reaction mixture was stirred at room temperature for 1 hr, and then AcOEt was added. The organic layer was washed three times with sodium phosphate buffer (pH ~ 4) and once with brine, dried over Na₂SO₄, and evaporated *in vacuo*. The residue was purified by column chromatography on silica gel (eluent: CH₂Cl₂/MeOH = 98/2 → 97/3) to afford **12** (0.26 g, 0.38 mmol) as a red solid in 74% yield. ¹H-

NMR (500 MHz, CD₃OD): δ 8.35 (d, 2H, J = 8.8 Hz), 7.96 (t, 1H, J = 5.2 Hz), 7.92 (d, 2H, J = 8.9 Hz), 7.88 (d, 2H, J = 7.5 Hz), 7.84 (d, 2H, J = 9.2 Hz), 7.71 (d, 2H, J = 7.4 Hz), 7.58 (d, 1H, J = 7.4 Hz), 7.41 (t, 2H, J = 7.5 Hz), 7.32 (t, 2H, J = 7.5 Hz), 6.88 (d, 2H, J = 9.2 Hz), 4.27 (d, 2H, J = 7.2 Hz), 4.21 (t, 1H, J = 6.7 Hz), 3.90 (m, 1H), 3.72 (t, 2H, J = 6.9 Hz), 3.04 (m, 5H), 2.38 (t, 2H, J = 6.8 Hz), 1.74–1.52 (m, 2H), 1.42–1.26 (m, 4H).

Fmoc Solid-Phase Synthesis of 13–23

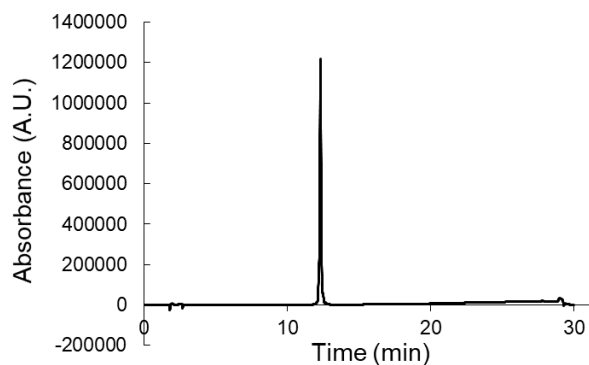
Fmoc-NH-Sieber resin was treated with 20% piperidine in DMF in a PD-10 column at room temperature for 10 min. Each assembly step was done by activating the Fmoc-amino acid with HBTU (0.038 mmol, condensation reagent), HOBT · H₂O (0.038 mmol, racemization suppressants) and DIEA (0.075 mmol) in DMF (0.80 mL) at room temperature for 60 min. Removal of the Fmoc group was done twice by using 20% pyridine in DMF (2.0 mL) at room temperature for 2 and 10 min.

For the condensation of the linker (**1**), to the resin were added **1**, HBTU (15 mg, 0.040 mmol), HOBT · H₂O (5.7 mg, 0.037 mmol) and DIEA (14 μ L, 0.081 mmol) in DMF (0.80 mL). The mixture was stirred at room temperature for 60 min, and then removal of the Fmoc group was done twice by using 20% pyridine in DMF (2.0 mL) at room temperature for 2 and 10 min. For the condensation of 5-FITC, to the resin were added 5-FITC and DIEA (17 μ L, 0.099 mmol) in DMF (0.80 mL). The mixture was stirred at room temperature for 60 min, and then the resin was washed with DMF. For the cleavage of the synthetic peptide without loss of side-chain-protecting groups, the resin was mixed with 1% TFA and 1% TES in CH₂Cl₂ (2.0 mL) at room temperature for 5 min (10 times). The filtrate was collected and evaporated to afford the crude intermediate.

To a solution of the crude intermediate was added TFA/CH₂Cl₂ (10 mL; 7/3). The reaction mixture was stirred at room temperature for 3 hr, and then evaporated. The residue was purified by reversed-phase HPLC to obtain **13–23**.

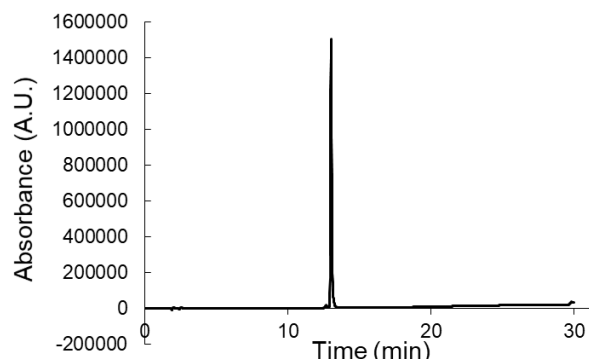
Synthesis of 13 (FITC-H4K16(Dab)-NH₂ (9 residues))

The solid-phase synthesis was performed on Fmoc-NH-Sieber resin (0.10 g, 52 μ mol). The Fmoc-amino acids, **1** (linker) and 5-FITC used in this synthesis were as follows: Fmoc-K(Boc)-OH (71 mg, 0.15 mmol), Fmoc-R(Pbf)-OH (99 mg, 0.15 mmol), Fmoc-H(Trt)-OH (95 mg, 0.15 mmol), Fmoc-R(Pbf)-OH (98 mg, 0.15 mmol), Fmoc-K(DabcyL-PH)-OH (99 mg, 0.15 mmol), Fmoc-A-OH (50 mg, 0.15 mmol), Fmoc-G-OH (45 mg, 0.15 mmol), Fmoc-G-OH (45 mg, 0.15 mmol), Fmoc-K(Boc)-OH (71 mg, 0.15 mmol), **1** (57 mg, 0.16 mmol) and 5-FITC (39 mg, 0.10 mmol). The residue was purified by reversed-phase HPLC to afford **13 (FITC-H4K16(Dab)-NH₂ (9 residues))** (12 mg, 6.4 μ mol) as a red solid in 12% yield. Purity by HPLC: 97.3% (254 nm); t_R = 12.3 min (A: B = 90: 10 \rightarrow 0: 100 (17 min); A: 0.1% TFA MilliQ, B: 0.1% TFA CH₃CN); HRMS (ESI⁺) calcd for C₈₈H₁₂₂N₂₆O₁₆S [M+H]⁺: 1830.92528; found: m/z = 1830.92615.



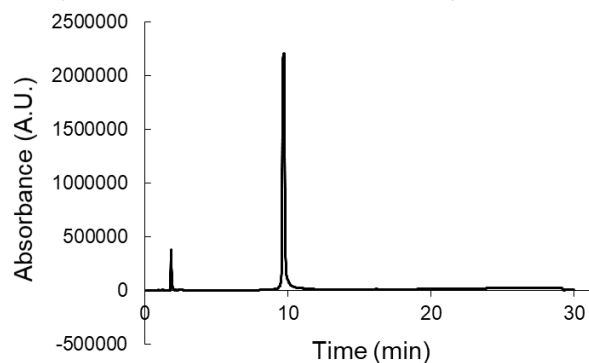
Synthesis of 14 (FITC-H4K16(DabcyL-PH)-NH₂ (7 residues))

The solid-phase synthesis was performed on Fmoc-NH-Sieber resin (98 mg, 51 μ mol). The Fmoc-amino acids, **1** (linker) and 5-FITC used in this synthesis were as follows: Fmoc-R(Pbf)-OH (99 mg, 0.15 mmol), Fmoc-H(Trt)-OH (97 mg, 0.16 mmol), Fmoc-R(Pbf)-OH (0.10 g, 0.15 mmol), Fmoc-K(DabcyI-PH)-OH (0.10 g, 0.16 mmol), Fmoc-A-OH (52 mg, 0.16 mmol), Fmoc-G-OH (48 mg, 0.16 mmol), Fmoc-G-OH (46 mg, 0.15 mmol), **1** (56 mg, 0.15 mmol) and 5-FITC (41 mg, 0.11 mmol). The residue was purified by reversed-phase HPLC to afford **14** (**FITC-H4K16(Dab)-NH₂** (**7 residues**)) (11 mg, 5.6 μ mol) as a red solid in 11% yield. Purity by HPLC: 96.3% (254 nm); t_R = 13.0 min (A: B = 90: 10 \rightarrow 0: 100 (17 min); A: 0.1% TFA MilliQ, B: 0.1% TFA CH₃CN); HRMS (ESI⁺) calcd for C₇₆H₉₈N₂₂O₁₄S [M+H]⁺: 1574.73535; found: m/z = 1574.73219.



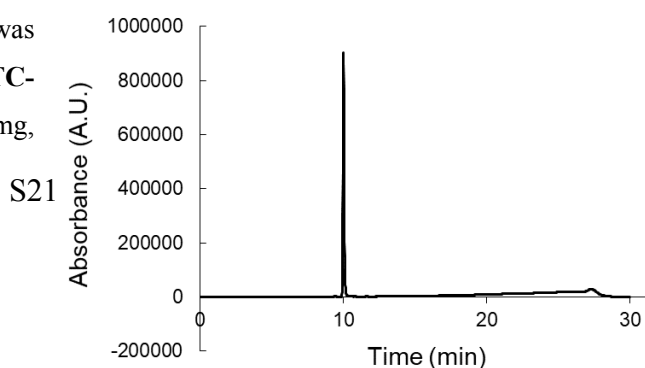
Synthesis of **15** (**FITC-H4K16(Dab)-NH₂** (**11 residues**))

The solid-phase synthesis was performed on Fmoc-NH-Sieber resin (25 mg, 13 μ mol). The Fmoc-amino acids, **1** (linker) and 5-FITC used in this synthesis were as follows: Fmoc-Val-OH (14 mg, 0.041 mmol), Fmoc-Lys(Boc)-OH (18 mg, 0.038 mmol), Fmoc-Arg(Pbf)-OH (26 mg, 0.040 mmol), Fmoc-His(Trt)-OH (25 mg, 0.040 mmol), Fmoc-Arg(Pbf)-OH (25 mg, 0.038 mmol), Fmoc-Lys(DabcyI-PH)-OH (26 mg, 0.041 mmol), Fmoc-Ala-OH (13 mg, 0.038 mmol), Fmoc-Gly-OH (11 mg, 0.038 mmol), Fmoc-Gly-OH (13 mg, 0.044 mmol), Fmoc-Lys(Boc)-OH (18 mg, 0.038 mmol), Fmoc-Gly-OH (12 mg, 0.041 mmol), **1** (14 mg, 0.039 mmol) and 5-FITC (10 mg, 0.026 mmol). The residue was purified by reversed-phase HPLC to afford **15** (**FITC-H4K16(DabcyI-PH)-NH₂** (**11 residues**)) (14 mg, 5.3 μ mol) as a dark red solid in 41% yield. Purity by HPLC: 98.7% (254 nm); t_R = 9.74 min (A: B = 90: 10 \rightarrow 0: 100 (17 min); A: 0.1% TFA MilliQ, B: 0.1% TFA CH₃CN); HRMS (ESI⁺) calcd for C₉₅H₁₃₄N₂₈O₁₈S [M+H]⁺: 1987.01516; found: m/z = 1987.01151.



Synthesis of **16** (**FITC-NFRIK(DabcyI-PH)RYSN-NH₂** (**9 residues**))

The solid-phase synthesis was performed on Fmoc-NH-Sieber resin (25 mg, 13 μ mol). The Fmoc-amino acids, **1** (linker) and 5-FITC used in this synthesis were as follows: Fmoc-Asn(Trt)-OH (22 mg, 0.037 mmol), Fmoc-Ser(tBu)-OH (14 mg, 0.037 mmol), Fmoc-Tyr(tBu)-OH (17 mg, 0.037 mmol), Fmoc-Arg(Pbf)-OH (24 mg, 0.037 mmol), Fmoc-Lys(DabcyI-PH)-OH (22 mg, 0.034 mmol), Fmoc-Ile-OH (13 mg, 0.037 mmol), Fmoc-Arg(Pbf)-OH (24 mg, 0.037 mmol), Fmoc-Phe-OH (15 mg, 0.039 mmol), Fmoc-Asn(Trt)-OH (22 mg, 0.037 mmol), **1** (14 mg, 0.038 mmol) and 5-FITC (10 mg, 0.026 mmol). The residue was purified by reversed-phase HPLC to afford **16** (**FITC-NFRIK(DabcyI-PH)RYSN-NH₂** (**9 residues**)) (16 mg,

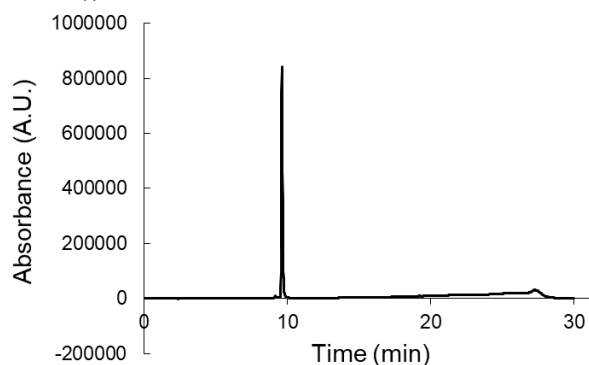


S21

7.2 μmol) as a red solid in 58% yield. Purity by HPLC: 98.8% (254 nm); $t_{\text{R}} = 10.0$ min (A: B = 80: 20 \rightarrow 0: 100 (20 min); A: 0.1% TFA MilliQ, B: 0.1% TFA CH_3CN); HRMS (ESI⁺) calcd for $\text{C}_{98}\text{H}_{126}\text{N}_{24}\text{O}_{20}\text{S}$ [M+H]⁺: 1990.93009; found: $m/z = 1990.92574$.

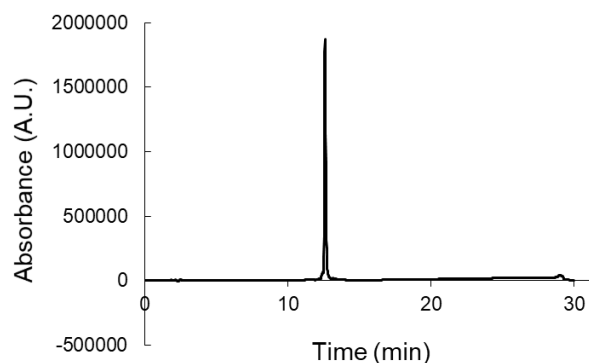
Synthesis of 17(FITC-DYRIK(DabcyI-PH)RYHT-NH₂ (9 residues))

The solid-phase synthesis was performed on Fmoc-NH-Sieber resin (25 mg, 13 μmol). The Fmoc-amino acids, **1** (linker) and 5-FITC used in this synthesis were as follows: Fmoc-Thr(tBu)-OH (15 mg, 0.038 mmol), Fmoc-His(Trt)-OH (14 mg, 0.023 mmol), Fmoc-Tyr(tBu)-OH (17 mg, 0.037 mmol), Fmoc-Arg(Pbf)-OH (24 mg, 0.037 mmol), Fmoc-Lys(DabcyI-PH)-OH (22 mg, 0.034 mmol), Fmoc-Ile-OH (13 mg, 0.037 mmol), Fmoc-Arg(Pbf)-OH (24 mg, 0.037 mmol), Fmoc-Tyr(tBu)-OH (17 mg, 0.037 mmol), Fmoc-Aso(tBu)-OH (16 mg, 0.039 mmol), **1** (14 mg, 0.038 mmol) and 5-FITC (10 mg, 0.026 mmol). The residue was purified by reversed-phase HPLC to afford **17 (FITC-DYRIK(DabcyI-PH)RYHT-NH₂ (9 residues))** (18 mg, 7.5 μmol) as a red solid in 60% yield. Purity by HPLC: 97.3% (254 nm); $t_{\text{R}} = 9.63$ min (A: B = 80: 20 \rightarrow 0: 100 (20 min); A: 0.1% TFA MilliQ, B: 0.1% TFA CH_3CN); HRMS (ESI⁺) calcd for $\text{C}_{101}\text{H}_{128}\text{N}_{24}\text{O}_{21}\text{S}$ [M+H]⁺: 2044.94065; found: $m/z = 2044.93862$.



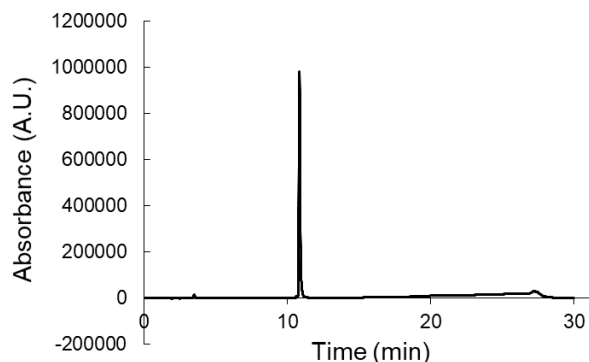
Synthesis of 18 (FITC-H4K16(DabcyI-BH)-NH₂ (9 residues))

The solid-phase synthesis was performed on Fmoc-NH-Sieber resin (24 mg, 13 μmol). The Fmoc-amino acids, **1** (linker) and 5-FITC used in this synthesis were as follows: Fmoc-Lys(Boc)-OH (18 mg, 0.039 mmol), Fmoc-Arg(Pbf)-OH (26 mg, 0.039 mmol), Fmoc-His(Trt)-OH (24 mg, 0.0390 mmol), Fmoc-Arg(Pbf)-OH (25 mg, 0.038 mmol), Fmoc-Lys(DabcyI-BH)-OH (25 mg, 0.038 mmol), Fmoc-Ala-OH (13 mg, 0.038 mmol), Fmoc-Gly-OH (11 mg, 0.038 mmol), Fmoc-Gly-OH (12 mg, 0.040 mmol), Fmoc-Lys(Boc)-OH (19 mg, 0.040 mmol), **1** (14 mg, 0.039 mmol) and 5-FITC (10 mg, 0.026 mmol). The residue was purified by reversed-phase HPLC to afford **18 (FITC-H4K16(DabcyI-BH)-NH₂ (9 residues))** (14 mg, 5.7 μmol) as a dark red solid in 46% yield. Purity by HPLC: 95.6% (254 nm); $t_{\text{R}} = 12.6$ min (A: B = 90: 10 \rightarrow 0: 100 (20 min); A: 0.1% TFA MilliQ, B: 0.1% TFA CH_3CN); HRMS (ESI⁺) calcd for $\text{C}_{89}\text{H}_{124}\text{N}_{26}\text{O}_{16}\text{S}$ [M+H]⁺: 1844.94093; found: $m/z = 1844.93841$.



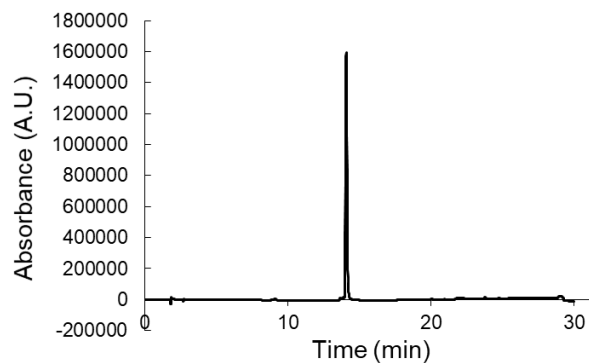
Synthesis of 19 (FITC-H4K16(Disperse Red)-NH₂ (9 residues))

The solid-phase synthesis was performed on Fmoc-NH-Sieber resin (25 mg, 13 μ mol). The Fmoc-amino acids, **1** (linker) and 5-FITC used in this synthesis were as follows: Fmoc-Lys(Boc)-OH (18 mg, 0.038 mmol), Fmoc-Arg(Pbf)-OH (24 mg, 0.037 mmol), Fmoc-His(Trt)-OH (23 mg, 0.037 mmol), Fmoc-Arg(Pbf)-OH (24 mg, 0.037 mmol), Fmoc-Lys(Disperse Red)-OH (25 mg, 0.037 mmol), Fmoc-Ala-OH (12 mg, 0.036 mmol), Fmoc-Gly-OH (12 mg, 0.040 mmol), Fmoc-Gly-OH (12 mg, 0.040 mmol), Fmoc-Lys(Boc)-OH (18 mg, 0.038 mmol), **1** (14 mg, 0.038 mmol) and 5-FITC (10 mg, 0.026 mmol). The residue was purified by reversed-phase HPLC to afford **19** (**FITC-H4K16(Disperse Red)-NH₂ (9 residues)**) (25 mg, 10 μ mol) as a dark red solid in 82% yield. Purity by HPLC: 98.0% (254 nm); t_R = 10.9 min (A: B = 90: 10 \rightarrow 0: 100 (20 min); A: 0.1% TFA MilliQ, B: 0.1% TFA CH₃CN); HRMS (ESI⁺) calcd for C₈₇H₁₁₉N₂₇O₁₈S [M+H]⁺: 1861.89471; found: m/z = 1861.89138.



Synthesis of **20** (**FITC-DYRIK(Disperse Red)RYHT-NH₂ (9 residues)**)

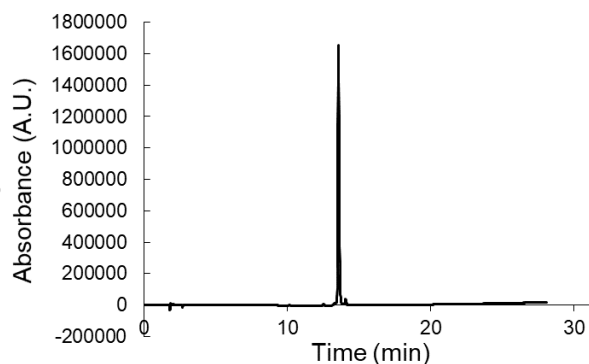
The solid-phase synthesis was performed on Fmoc-NH-Sieber resin (25 mg, 13 μ mol). The Fmoc-amino acids, **1** (linker) and 5-FITC used in this synthesis were as follows: Fmoc-Thr(tBu)-OH (15 mg, 0.038 mmol), Fmoc-His(Trt)-OH (14 mg, 0.023 mmol), Fmoc-Tyr(tBu)-OH (17 mg, 0.037 mmol), Fmoc-Arg(Pbf)-OH (24 mg, 0.037 mmol), Fmoc-Lys(Disperse Red)-OH (22 mg, 0.032 mmol), Fmoc-Ile-OH (13 mg, 0.037 mmol), Fmoc-Arg(Pbf)-OH (24 mg, 0.037 mmol), Fmoc-Tyr(tBu)-OH (17 mg, 0.037 mmol), Fmoc-Asp(tBu)-OH (16 mg, 0.039 mmol), **1** (14 mg, 0.038 mmol) and 5-FITC (10 mg, 0.026 mmol). The residue was purified by reversed-phase HPLC to afford **20** (**FITC-DYRIK(Disperse Red)RYHT-NH₂ (9 residues)**) (16 mg, 6.4 μ mol) as a dark red solid in 51% yield. Purity by HPLC: 96.1% (254 nm); t_R = 14.1 min (A: B = 90: 10 \rightarrow 0: 100 (20 min); A: 0.1% TFA MilliQ, B: 0.1% TFA CH₃CN); HRMS (ESI⁺) calcd for C₁₀₀H₁₂₅N₂₅O₂₃S [M+H]⁺: 2075.91008; found: m/z = 2075.90814.



Synthesis of **21** (**FITC-RalB(Disperse Red)-NH₂ (9 residues)**)

The solid-phase synthesis was performed on Fmoc-NH-Sieber resin (25 mg, 13 μ mol). The Fmoc-amino acids, **1** (linker) and 5-FITC used in this synthesis were as follows: Fmoc-Ser(tBu)-OH (15 mg, 0.039 mmol), Fmoc-Ser(tBu)-OH (15 mg, 0.039 mmol), Fmoc-Arg(Pbf)-OH (24 mg, 0.037 mmol), Fmoc-Glu(tBu)-OH (17 mg, 0.040 mmol), Fmoc-Lys(Disperse Red)-OH (22 mg, 0.032 mmol), Fmoc-Phe-OH (15 mg, 0.039 mmol), Fmoc-Ser(tBu)-OH (15 mg, 0.039 mmol), Fmoc-Lys(Boc)-OH (18 mg, 0.038 mmol), Fmoc-Lys(Boc)-OH (18 mg, 0.038 mmol), **1** (14 mg, 0.038 mmol) and 5-FITC (10 mg, 0.026 mmol). The residue was purified by reversed-phase HPLC to afford **21** (**FITC-RalB(Disperse Red)-NH₂ (9 residues)**) (12 mg,

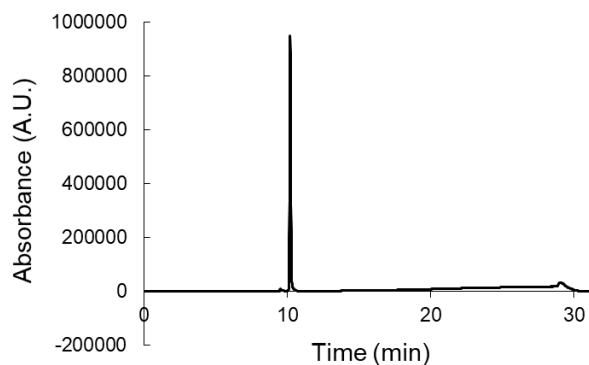
S23



5.4 μmol) as a dark red solid in 43% yield. Purity by HPLC: 95.3% (254 nm); $t_R = 13.6$ min (A: B = 90: 10 \rightarrow 0: 100 (20 min); A: 0.1% TFA MilliQ, B: 0.1% TFA CH_3CN); HRMS (ESI⁺) calcd for $\text{C}_{91}\text{H}_{120}\text{N}_{22}\text{O}_{23}\text{S}$ [M+H]⁺: 1920.86173; found: $m/z = 1920.85994$.

Synthesis of 22 (FITC-H2BK12(Disperse Red)-NH₂ (9 residues))

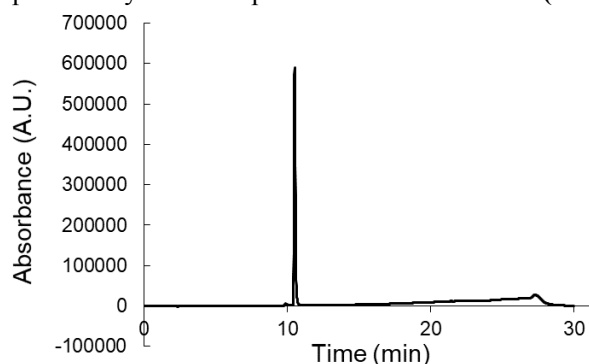
The solid-phase synthesis was performed on Fmoc-NH-Sieber resin (25 mg, 13 μmol). The Fmoc-amino acids, **1** (linker) and 5-FITC used in this synthesis were as follows: Fmoc-Lys(Boc)-OH (18 mg, 0.038 mmol), Fmoc-Ser(tBu)-OH (15 mg, 0.039 mmol), Fmoc-Gly-OH (12 mg, 0.040 mmol), Fmoc-Lys(Boc)-OH (18 mg, 0.038 mmol), Fmoc-Lys(Disperse Red)-OH (25 mg, 0.037 mmol), Fmoc-Pro-OH (14 mg, 0.039 mmol), Fmoc-Ala-OH (12



mg, 0.036 mmol), Fmoc-Pro-OH (14 mg, 0.039 mmol), Fmoc-Ala-OH (12 mg, 0.036 mmol), **1** (14 mg, 0.038 mmol) and 5-FITC (10 mg, 0.026 mmol). The residue was purified by reversed-phase HPLC to afford **22 (FITC-H2BK12(Disperse Red)-NH₂ (9 residues))** (22 mg, 11 μmol) as a dark red solid in 91% yield. Purity by HPLC: 97.0% (254 nm); $t_R = 10.2$ min (A: B = 80: 20 \rightarrow 0: 100 (20 min); A: 0.1% TFA MilliQ, B: 0.1% TFA CH_3CN); HRMS (ESI⁺) calcd for $\text{C}_{83}\text{H}_{109}\text{N}_{19}\text{O}_{19}\text{S}$ [M+H]⁺: 1707.78678; found: $m/z = 1707.78458$.

Synthesis of 23 (FITC-H3K9(Disperse Red)-NH₂ (9 residues))

The solid-phase synthesis was performed on Fmoc-NH-Sieber resin (25 mg, 13 μmol). The Fmoc-amino acids, **1** (linker) and 5-FITC used in this synthesis were as follows: Fmoc-Gly-OH (12 mg, 0.040 mmol), Fmoc-Gly-OH (12 mg, 0.040 mmol), Fmoc-Thr(tBu)-OH (15 mg, 0.038 mmol), Fmoc-Ser(tBu)-OH (15 mg, 0.039 mmol), Fmoc-Lys(Disperse Red)-OH (25 mg, 0.037 mmol), Fmoc-Arg(Pbf)-OH (24 mg, 0.037 mmol), Fmoc-Ala-OH (12 mg, 0.036 mmol), Fmoc-Thr(tBu)-OH (15 mg, 0.038 mmol), Fmoc-Glu(Trt)-OH (23 mg, 0.038 mmol), **1** (14 mg, 0.038 mmol) and 5-FITC (10 mg, 0.026 mmol). The residue was purified by reversed-phase HPLC to afford **23 (FITC-H3K9(Disperse Red)-NH₂ (9 residues))** (14 mg, 7.4 μmol) as a red solid in 59% yield. Purity by HPLC: 96.1% (254 nm); $t_R = 10.6$ min (A: B = 80: 20 \rightarrow 0: 100 (20 min); A: 0.1% TFA MilliQ, B: 0.1% TFA CH_3CN); HRMS (ESI⁺) calcd for $\text{C}_{79}\text{H}_{102}\text{N}_{21}\text{O}_{22}\text{S}$ [M+H]⁺: 1728.72290; found: $m/z = 1728.72429$.



***In vitro* assay**

Preparation of SIRT assay buffer

SIRT assay buffer was prepared at the time of use by adding 1 M DTT (final concentration: 2 mM) and 10% Triton X-100 (final concentration: 0.05%) to Tris-buffer (100 mM Tris-HCl (pH 8.0) and 150 mM NaCl).

Absorption and fluorescence spectroscopy

Absorption and fluorescence spectra were measured in a quartz cuvette (4 × 4 × 40 mm) on UV1800 (Shimadzu, Japan) and RF5300PC (Shimadzu, Japan) instruments, respectively. The spectra of SIRT probes were measured in Tris-buffer (100 mM Tris-HCl (pH 8.0), 150 mM NaCl) at the final concentration of 1 μM (0.01% DMSO). The excitation wavelength was 490 nm. Relative fluorescence quantum yield was obtained by comparing the area under the emission spectrum of the sample in Tris-buffer (pH 8.0) with that of fluorescein in 0.1 N NaOH (quantum yield 0.85).

Enzymatic reaction of SIRT probes and SIRTs on 96-well microplates

Enzymatic assay was performed on Corning 96-well half-area plates (#3694) using essentially the same procedure as that employed with the fluorometer. Enzymatic reactions were performed in *SIRT assay buffer* containing SIRT probes (2.5 μM, 0.25% DMSO), NAD⁺ (500 μM) with or without NAM (100 μM). SIRTs (35 nM) were added last. The total assay volume was 40 μL. The fluorescence intensity was measured at 37°C every 5 min for 1 hr with an ARVO X5 plate reader (filters: Ex = 485 nm, Em = 535 nm). Experiments were done at least in triplicate, and results are shown as mean ± S.D.

Determination of kinetic parameters with SIRT1–3 (K_m and k_{cat} of SIRT probes) using a plate reader

Enzymatic assay was performed with Corning 96-well half-area plates (#3694). Enzymatic reactions were performed in *SIRT assay buffer* containing SIRT probes. Probe concentrations were as follows. With SIRT1: **18**: final 3.125, 6.25, 12.5 and 25 μM, **14**: final 0.3125, 0.625, 1.25, 2.5, 5 and 10 μM, **16**: final 0.25, 0.5, 1, 2 and 4 μM, **19**: final 0.125, 0.25, 0.5, 1, 2 and 4 μM, **15**, **20–23**: final 0.03125, 0.0625, 0.125, 0.25, 0.5 and 1 μM, **13**: final 0.125, 0.25, 0.5 and 1 μM, **17**: final 0.25, 0.5 and 1 μM. With SIRT2: **13**, **14**, **16**, **17**: final 0.125, 0.25, 0.5, 1, 2 and 4 μM; **15**, **18–23**: final 0.03125, 0.0625, 0.125, 0.25, 0.5 and 1 μM. With SIRT3: **13**, **14**, **16–18**, **19**: final 0.125, 0.25, 0.5, 1, 2 and 4 μM; **20–23**: final 0.0625, 0.125, 0.25, 0.5, 1 and 2 μM, **15**: final 0.03125, 0.0625, 0.125, 0.25, 0.5 and 1 μM (1% DMSO), 500 μM NAD⁺. SIRTs (35 nM) were added last. The total assay volume was 40 μL. The fluorescence intensity was measured at 37 °C every 1 min for 40 min with an ARVO X5 plate reader (filters: Ex = 485 nm, Em = 535 nm). The initial velocity (μM/sec) of the enzymatic reaction between 10 min and 20 min after addition of SIRT was calculated and plotted against SIRT probe concentration. Experiments were run at least in triplicate, and the results are shown as mean ± S.D. The points were fitted to a Michaelis-Menten curve by using GraphPad Prism6.

Evaluation of the linearity of the enzymatic reaction of 18 with SIRT2

Enzymatic reactions were performed in *SIRT assay buffer* containing **18** (final 1 μM) and NAD⁺ (final 500 μM). SIRT2 (final 1.09–35.0 nM) was added last. The total assay volume was 20 μL. The assay plate was incubated for 2

hr at room temperature, and the fluorescence intensity was measured at the indicated time points with an ARVO X5 plate reader (filters: Ex = 485 nm, Em = 535 nm). Results are mean \pm S.D.

Optimization of enzyme concentration for HTS with 18

Enzymatic reactions were performed in *SIRT assay buffer* containing **18** (final 1 μ M), NAD⁺ (final 500 μ M). SIRT2 (final 2.92–8.75 nM) was added last. The total assay volume was 20 μ L. The assay plate was incubated for 4 hr at room temperature, and the fluorescence intensity was measured at 1 hr intervals with an ARVO X5 plate reader (filters: Ex = 485 nm, Em = 535 nm). Results are mean \pm S.D.

Calculation of screening validation factors

Enzymatic reactions were performed in *SIRT assay buffer* containing **18** (1 μ M) and NAD⁺ (500 μ M). SIRT2 (2.92 nM) were added last. The total assay volume was 20 μ L. The assay plate was incubated for 2 hr at room temperature, and the fluorescence intensity was measured at the indicated time points with an ARVO X5 (filters: Ex = 485 nm, Em = 535 nm). Results are mean \pm S.D. The following values were calculated:

Coefficient of variation CV (%) = standard deviation (SD)/average (Av).

Signal/background ratio (S/B) = $Av_{100\%}/Av_{0\%}$.

Signal/noise ratio (S/N) = $(Av_{100\%}-Av_{0\%})/SD_{0\%}$

Z' factor = $Z' = 1 - (3 \times SD_{100\%} + 3 \times SD_{0\%}) / (Av_{100\%} - Av_{0\%})$

where $Av_{100\%}$ is the average fluorescence intensity of forty 100% activity samples (i.e., with SIRT2). $Av_{0\%}$ is the average fluorescence intensity of eight 0% activity samples (i.e., without SIRT2).

Determination of IC₅₀ value of S2DMi-6 with SIRT2 using 18

S2DMi-6 was dissolved in DMSO, and diluted as required with *SIRT assay buffer* (10 μ L, final 0.122–250 nM (0.25% DMSO)). Enzymatic reactions were performed in *SIRT assay buffer* containing a pre-mixture (20 μ L) of **18** (2 μ M, final 1 μ M) and NAD⁺ (1 mM, final 500 μ M) with SIRT2 (35 nM, 10 μ L, final 8.75 nM). The total assay volume was 40 μ L. The plates were incubated at room temperature for 2 hr, and the fluorescence intensity was measured with an ARVO X5 plate reader (filters: Ex = 485/14 nm, Em = 535/25 nm). Experiments were done at least in triplicate, and results are shown as mean \pm SD. IC₅₀ values were calculated by using GraphPad Prism6.

Determination of IC₅₀ value of S2DMi-9 with SIRT6 using 23

S2DMi-9 was dissolved in DMSO, and diluted as required with *SIRT assay buffer* (10 μ L, final 0.0195–2.5 μ M (1% DMSO)). Enzymatic reactions were performed in *SIRT assay buffer* containing a pre-mixture (20 μ L) of **23** (2 μ M, final 1 μ M) and NAD⁺ (1 mM, final 500 μ M) with SIRT6 (194 nM, 10 μ L, final 48.6 nM). The total assay volume was 40 μ L. The plates were incubated at room temperature for 2 hr, and the fluorescence intensity was measured with an ARVO X5 plate reader (filters: Ex = 485/14 nm, Em = 535/25 nm). Experiments were done at least in triplicate, and results are shown as mean \pm SD. IC₅₀ values were calculated by using GraphPad Prism6.

SIRT2 inhibitor screening

For primary screening, high-throughput screening (HTS) of 9600 compounds from the chemical library of Drug Discovery Initiative, The University of Tokyo was performed. First, prepared solutions (2 mM in DMSO, 50 nL, final 10 μ M (0.5% DMSO)) of test compounds were dispensed into 384-well microplates (320 compounds/plate, total 30 plates). Next, a pre-mixture (5 μ L) of **18** (2 μ M, final 1 μ M) and NAD⁺ (1 mM, final 500 μ M) dissolved in *SIRT assay buffer* was dispensed into each well of the assay plates. Finally, SIRT2 solution (5.83 nM, 5 μ L, final 2.92 nM) dissolved in *SIRT assay buffer* was dispensed (total volume was 10 μ L), and the plates were incubated at room temperature for 2 h. The fluorescence was measured ($\lambda_{\text{ex}} = 485$ nm, $\lambda_{\text{em}} = 535$ nm) with a microplate reader (ARVO X5). Control wells, i.e., no enzyme wells, no compound wells, and **S2DMi-6** (20 μ M in DMSO, 50 nL, final 100 nM (0.5% DMSO)) wells as positive controls ($n = 16$ each), were included in all plates. From the results, we calculated CV (coefficient of variation) = $\text{SD}/\text{Av} \leq 10\%$; S/B = signal/background ≥ 3.0 ; S/N = signal/noise; Z' factor = $1 - (3 \times \text{SD}_{100\%} + 3 \times \text{SD}_{0\%}) / (\text{Av}_{100\%} - \text{Av}_{0\%}) \geq 0.5$ for each plate as described above. SD = standard deviation, Av = average.

Evaluation of SIRT2-inhibitory activity by means of assay with 18

Compounds **A**, **B** and **C** were dissolved in DMSO, and the solutions were diluted as required with *SIRT assay buffer* (10 μ L, final 3.125, 6.25, 12.5, 25, 50, 100 μ M (1% DMSO)). Enzymatic reactions were performed in *SIRT assay buffer* containing a pre-mixture (0 μ L) of **18** (2 μ M, final 1 μ M) and NAD⁺ (1 mM, final 500 μ M) with SIRT2 (11.7 nM, 10 μ L, final 2.92 nM). The total assay volume was 40 μ L. The plates were incubated at room temperature for 2 h, and the fluorescence intensity was measured with an ARVO X5 plate reader (filters: $E_x = 485/14$ nm, $E_m = 535/25$ nm). Experiments were done at least in triplicate, and results are shown as mean \pm SD. IC₅₀ values were calculated by using GraphPad Prism6.

Evaluation of SIRT2-inhibitory activity by means of assay with p53(Myristic)-AMC

Compounds **A**, **B** and **C** were dissolved in DMSO, and the solutions were diluted as required with *SIRT assay buffer* (5 μ L, final 3.125, 6.25, 12.5, 25, 50, 100 μ M (1% DMSO)). Enzymatic reactions were performed in *SIRT assay buffer* containing **p53(Myristic)-AMC** (4 μ M, 5 μ L, final 1 μ M) and NAD⁺ (2 mM, 5 μ L, final 500 μ M) with SIRT2 (280 nM, 5 μ L, final 70 nM). The total assay volume was 20 μ L. The plates were incubated at room temperature for 3 h, and then a solution (20 μ M) of trypsin (final 100 nM) and nicotinamide (final 1 mM) in *SIRT assay buffer* was added. Fluorescence intensity was measured at 5 min intervals with an ARVO X5 plate reader (filters: $E_x = 355/40$ nm, $E_m = 460/25$ nm) for 20 min at 37°C. Experiments were done at least in triplicate, and results are shown as mean \pm SD. IC₅₀ values were calculated by using GraphPad Prism6.

Evaluation of SIRT2-inhibitory activity by means of assay with FLUOR DE LYS SIRT2 Kit

Compound **C** was dissolved in DMSO, and the solutions were diluted as required with *sirtuin assay buffer II* (50 mM Tris-HCl (pH 8.0), containing 137 mM NaCl, 2.7 mM KCl, 1 mM MgCl₂, 1 mg/mL bovine serum albumin (BSA)) (5 μ L, final 0.0488–100 μ M (0.5% DMSO)). Enzymatic reactions were performed in *sirtuin assay buffer II* containing **deacetylase substrate** (200 μ M, 5 μ L, final 50 μ M) and NAD⁺ (2 mM, 5 μ L, final 500 μ M) with SIRT2 (8 U, 5 μ L, final 2 U). The total assay volume was 20 μ L. The plates were incubated at room temperature for 2 h, and then a

solution (20 μ M) of Developer II and nicotinamide (final 2 mM) in *sirtuin assay buffer II* was added. Fluorescence intensity was measured at 5 min intervals with an ARVO X5 plate reader (filters: $E_x = 355/40$ nm, $E_m = 460/25$ nm) for 20 min at 37°C. Experiments were done at least in triplicate, and results are shown as mean \pm SD. IC_{50} values were calculated by using GraphPad Prism6.

Evaluation of SIRT1 and 3-inhibitory activity by means of assay with 18

Compound **C** was dissolved in DMSO, and the solutions were diluted as required with *SIRT assay buffer* (200 μ M, 10 μ L, final 50 μ M (1% DMSO)). Enzymatic reactions were performed in *SIRT assay buffer* containing a pre-mixture (20 μ L) of **18** (2 μ M, final 1 μ M) and NAD^+ (1 mM, final 500 μ M) with SIRT1 (1.50 nM, 10 μ L, final 0.375 nM) or SIRT3 (23.9 nM, 10 μ L, final 5.98 nM). The total assay volume was 40 μ L. The plates were incubated at room temperature for 2 h, and the fluorescence intensity was measured with an ARVO X5 plate reader (filters: $E_x = 485/14$ nm, $E_m = 535/25$ nm). Experiments were done at least in triplicate, and results are shown as mean \pm SD.

Evaluation of SIRT6-inhibitory activity by means of assay with 23

Compound **C** was dissolved in DMSO, and the solutions were diluted as required with *SIRT assay buffer* (200 μ M, 10 μ L, final 50 μ M (1% DMSO)). Enzymatic reactions were performed in *SIRT assay buffer* containing a pre-mixture (20 μ L) of **23** (2 μ M, final 1 μ M) and NAD^+ (1 mM, final 500 μ M) with SIRT6 (194 nM, 10 μ L, final 48.6 nM). The total assay volume was 40 μ L. The plates were incubated at room temperature for 2 h, and the fluorescence intensity was measured with an ARVO X5 plate reader (filters: $E_x = 485/14$ nm, $E_m = 535/25$ nm). Experiments were done at least in triplicate, and results are shown as mean \pm SD.

Determination of IC_{50} value of known small-molecular SIRT inhibitors with SIRT2 using 18

Nicotinamide, **AGK2**, **SirReal2** and **TM** were dissolved in DMSO, and diluted as required with *SIRT assay buffer* (10 μ L, final 0.0488–100 μ M (1% DMSO)), respectively. Enzymatic reactions were performed in *SIRT assay buffer* containing a pre-mixture (20 μ L) of **18** (2 μ M, final 1 μ M) and NAD^+ (1 mM, final 500 μ M) with SIRT2 (35 nM, 10 μ L, final 8.75 nM). The total assay volume was 40 μ L. The plates were incubated at room temperature for 2 hr, and the fluorescence intensity was measured with an ARVO X5 plate reader (filters: $E_x = 485/14$ nm, $E_m = 535/25$ nm). Experiments were done at least in triplicate, and results are shown as mean \pm SD. IC_{50} values were calculated by using GraphPad Prism6.

References for Supporting Information

- (S1) Kawaguchi, M.; Ikegawa, S.; Ieda, N.; Nakagawa, H. A fluorescent probe for imaging sirtuin activity in living cells, based on one-step cleavage of the Dabcyl quencher. *ChemBioChem* **2016**, *17*, 1961–1967.
- (S2) Anthony, A.; Schramm, V. L. Sir2 regulation by nicotinamide results from switching between base exchange and deacetylation chemistry. *Biochemistry*. **2003**, *42*, 9249–9256.
- (S3) Outeiro, T. F.; Kontopoulos, E.; Altmann, S. M.; Kufareva, I.; Strathearn, K. E; Amore, A. M.; Volk, C. B.; Maxwell, M. M.; Rochet, J-C.; McLean, P. J.; Young, A. B.; Abagyan, R.; Feany, M. B.; Hyman, B. T.; Kazantsev,

A. G. Sirtuin 2 inhibitors rescue alpha-synuclein-mediated toxicity in models of Parkinson's disease. *Science*. **2007**, *317*, 516–519.

(S4) Rumpf, T.; Schiedel, M.; Karaman, B.; Roessler, C.; North, B. J.; Lehotzky, A.; Oláh, J.; Ladwein, K. I.; Schmidtkunz, K.; Gajer, M.; Pannek, M.; Steegborn, C.; Sinclair, D. A.; Gerhardt, S.; Ovádi, J.; Schutkowski, M.; Sippl, W.; Einsle, O.; Jung, M. Selective Sirt2 inhibition by ligand-induced rearrangement of the active site. *Nat. Commun.* **2015**, *6*, 6263.

(S5) Jing, H.; Hu, J.; He, B.; Negrón Abril, Y. L.; Stupinski, J.; Weiser, K.; Carbonaro, M.; Chiang, Y.-L. Southard, T.; Giannakakou, P.; Weiss, R. S.; Lin, H. A SIRT2-selective inhibitor promotes c-Myc oncoprotein degradation and exhibits broad anticancer activity. *Cancer Cell*, **2016**, *29*, 767–768.

(S6) Kawaguchi, M.; Ieda, N.; Nakagawa, H. Development of peptide-based sirtuin defatty-acylase inhibitors identified by the fluorescence probe, SFP3, that can efficiently measure defatty-acylase activity of sirtuin. *J. Med. Chem.* **2019**, *62*, 5434–5452.